Potent Reversible Inhibitors of the Protein Tyrosine Phosphatase CD45

Rebecca A. Urbanek,* Suzanne J. Suchard,† Gary B. Steelman, Katharine S. Knappenberger, Linda A. Sygowski, Chris A. Veale, and Marc J. Chapdelaine

AstraZeneca Pharmaceuticals, 1800 Concord Pike, Wilmington, Delaware 19850

Received October 17, 2000

The cytosolic portion of CD45, a major transmembrane glycoprotein found on nucleated hematopoietic cells, contains protein tyrosine phosphatase activity and is critical for T-cell receptor-mediated T-cell activation. CD45 inhibitors could have utility in the treatment of autoimmune disorders and organ graft rejection. A number of 9,10-phenanthrenediones were identified that reversibly inhibited CD45-mediated *p*-nitrophenyl phosphate (*p*NPP) hydrolysis. Chemistry efforts around the 9,10-phenanthrenedione core led to the most potent inhibitors known to date. In a functional assay, the compounds were also potent inhibitors of T-cell receptor-mediated proliferation, with activities in the low micromolar range paralleling their enzyme inhibition. It was also discovered that the nature of modification to the phenanthrenedione pharmacophore could affect selectivity for CD45 over PTP1B (protein tyrosine phosphatase 1B) or vice versa.

Introduction

Inappropriate lymphocyte and monocyte/macrophage activation are an underlying cause of organ transplant rejection and autoimmune diseases such as multiple sclerosis and rheumatoid arthritis. Unfortunately, current therapies targeted at reducing immune-cell activation in these diseases also affect cells outside the immune system and consequently carry the liability of toxic side effects. For example, the immunosuppressants cyclosporine and FK506, which inhibit IL-2 production in T-cells by blocking the phosphatase activity of calcineurin, can also cause renal toxicity, neurotoxicity, and the increased risk of malignancy.[1−3] Rapamycin inhibits T-cell proliferation farther down the signaling pathway by inhibiting the autocrine response of T-cells to IL-2 by binding to and blocking a kinase essential for cell cycle progression.[4] In contrast to cyclosporine and FK506, rapamycin's antiproliferative effects are not limited to cells of the immune system and can affect growth factor-induced proliferation of fibroblasts, endothelial cells, hepatocytes, and smooth muscle cells.[5] Recent trials in renal transplantation reported an increased incidence of hypertriglyceridemia, hypercholesterolemia, thrombocytopenia, and leukopenia with sirolimus (rapamycin) treatment.[6] In addition, some psoriasis patients developed capillary leak syndrome following oral administration of sirolimus.[7] Thus, even though rapamycin represents a different class of immunosuppressive agent, it is not without significant toxicity.[7,8] Immunosuppressive drugs that more specifically target the signaling pathways in the hematopoietic cells responsible for initiating and maintaining inflammation should have fewer and/or different side effects than cyclosporine, FK506, or rapamycin.

The protein tyrosine phosphatases (PTPs) are a diverse family of enzymes that, together with the protein tyrosine kinases (PTKs), control the level of intracellular tyrosine phosphorylation, thus regulating many cellular functions.[9] The PTKs are responsible for phosphorylating tyrosine residues and were previously believed to be the only critical players in controlling levels of tyrosine phosphorylation. The PTPs are responsible for dephosphorylating these phosphotyrosine residues, and in the past decade great advances have been made in understanding the important role the PTPs play in maintaining the balance of tyrosine phosphorylation. Currently approximately 100 PTPs are known, and it has been predicted that as many as 500 PTP genes exist in the human genome.[10] The PTP family is recognized by an invariant amino acid signature motif present at the active site, (H/V)**C**$(X)_5$**R**(S/T), where the cysteine and arginine residues are essential for catalytic activity. Three-dimensional structural data show there are conserved structural elements such as the PTP motif and a conserved aspartic acid residue on a surface loop, but there is little primary sequence similarity in the PTP family.[11]

Although there is little sequence similarity, the PTPs do utilize the same mechanism of dephosphorylation, which involves the formation of a covalent thiophosphate intermediate by the invariant cysteine residue in the PTP signature motif. The invariant arginine residue in the PTP motif plays a role in substrate binding and transition state stabilization, and the invariant aspartic acid residue on the surface loop may act as a general acid in the first step and a general base in the second step, Figure 1.[11]

CD45 is a family of transmembrane PTPs that are expressed exclusively by hematopoietic cells. CD45 plays a critical role in T-cell receptor (TCR)-mediated signaling by regulating the phosphorylation and activity of src-family protein tyrosine kinases and their substrates.[12] The cytoplasmic domain of CD45 possesses the tyrosine phosphatase activity and is capable of dephosphorylating the negative regulatory site on $p56^{lck}$ and

* To whom correspondence should be addressed: Tel: 302-886-4818. Fax: 302-886-5382. E-mail: rebecca.urbanek@astrazeneca.com.

† Present Address: Bristol-Myers Squibb Pharmaceutical Research Institute, Immunology, Inflammation and Pulmonary Discovery, P.O. Box 4000, Princeton, NJ 08543-4000.

10.1021/jm000447i CCC: $20.00
Published on Web 05/02/2001

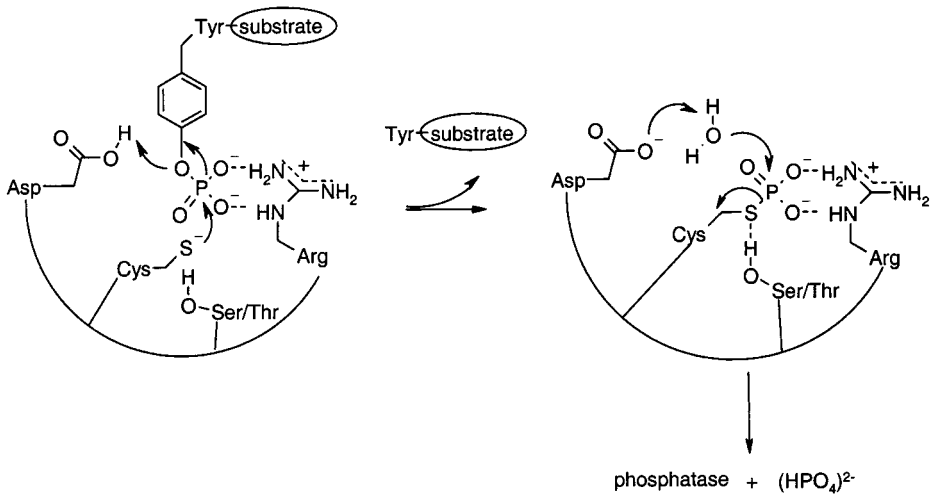

Figure 1. Dephosphorylation mechanism of the PTPs.

p59^{fyn} src kinases.[13] This allows the autophosphorylation of the positive regulatory site on these molecules and propagation of TCR-mediated signaling. CD45 can also associate with cell surface receptors that lack a transmembrane domain and may work in concert with these receptors to transduce an activation signal.[14,15] Blockade of CD45 by anti-CD45 antibodies inhibits T-cell activation in vitro,[16] and T-cells from CD45 KO mice fail to respond to antigen challenge.[12]

Recently, Lazarovits et al.[17] reported that a monoclonal antibody against the RB isoform of CD45 inhibits the alloreactivity of human CD4$^+$ lymphocytes in vitro and prevents renal and pancreatic islet rejection in mice.[18,19] Furthermore, lymphocytes from antibody-treated animals showed reduced levels of steady state mRNA transcripts for IFN-γ, TNFα, and ICAM-1. These studies highlight the potential value of selective small-molecule inhibitors of CD45 in the treatment of transplant rejection and autoimmune diseases.

Development of potent small-molecule PTP inhibitors is in its infancy, but it is an area of increased interest due to a growing list of important physiological roles played by many PTPs.[11] To date, the majority of early PTP inhibitors are compounds with a nonhydrolyzable phosphotyrosine mimic, which may or may not be incorporated into a peptide scaffold.[20−34] The negatively charged phosphoryl mimic would be expected to make cell permeability difficult.[35] The peptide portion of these inhibitors would be expected to be metabolically labile in vivo.

The availability of crystal structures of protein tyrosine phosphatase 1B (PTP1B) has facilitated the development of small-molecule PTP1B inhibitors.[35−40] PTP1B has been shown to be a negative regulator of the insulin receptor, thus its inhibition could be therapeutically useful in the treatment of diabetes and obesity.[41] In the present report, we describe our efforts leading to potent and selective inhibitors of CD45.

Identification of Lead Series and Scope of Early SAR

High-throughput screening of an archival collection of compounds utilizing the cytosolic portion of CD45 and *p*-nitrophenyl phosphate (*p*NPP) as the substrate afforded the compounds shown in Figure 2 that were

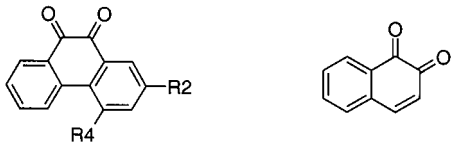

1, $R^2 = R^4 = H$
2, $R^2 = Br$
3, $R^2 = NH_2$
4, $R^2 = NO_2$
5, $R^4 = NO_2$

6

Figure 2. Hits in the high-throughput screen.

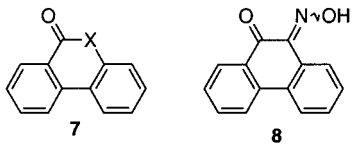

7
X = N, O

8

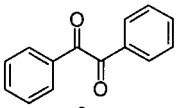

9

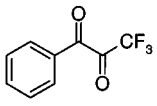

10

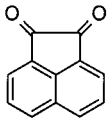

11

Figure 3. Structurally related inactive compounds.

active in the range of 400−2000 nM with parallel functional activity inhibiting T-cell proliferation in the range of 300−1600 nM. The antiproliferative effect was shown not to be due to cytotoxicity.

The required presence of a 1,2-dione embedded in a six-membered ring to maintain the desired inhibitory activity became evident upon survey of similar readily available compounds (Figure 3). A number of compounds of type **7**, where the central dione-containing ring of 9,10-phenanthrenedione was replaced with a lactone or lactam, were tested but no CD45 inhibition was observed at 10 μM. The mono-oxime of 9,10-phenanthrenedione, **8**, was also tested, and again no inhibition of CD45 was observed. Benzil and several of its derivatives, including compounds which contained electron-withdrawing groups, and other 1,2-diones (compounds of type **9** and **10**) were void of CD45 inhibitory activity at 10 μM. Simple phenanthrene and 1,2-dioxoacenaphthene **11** failed to inhibit *p*NPP hydrolysis by CD45.

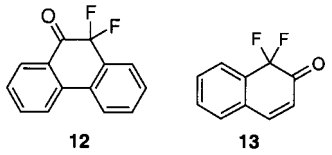

Figure 4. Inactive α-difluoro compounds.

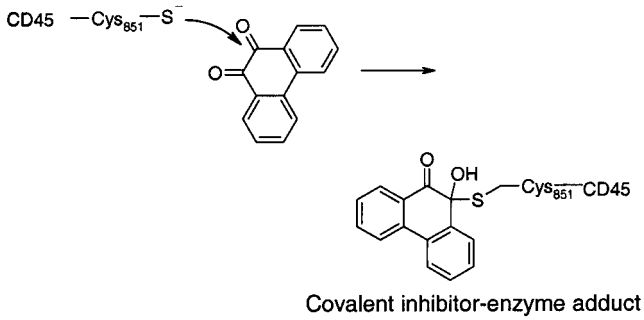

Figure 5. Hypothesized inhibitory mechanism.

Scheme 1. Synthesis of 4-Aryl-1,2-naphthalenediones[a]

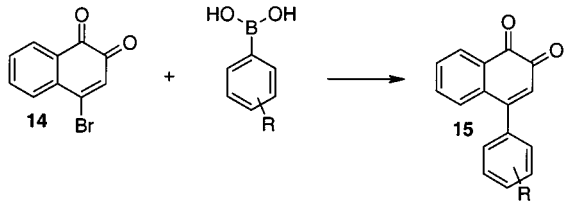

[a] Reagents: Pd_2dba_3, P(*o*-tol)$_3$, K_2CO_3, 20% H_2O−THF, reflux.

Twelve different 4-amino-1,2-naphthalenediones were evaluated and were shown to be inactive against CD45 at 10 μM. Furthermore, evaluation of a set of 1,4-naphthalenediones did not lead to compounds of sufficient activity to warrant further investigation.

The known α-difluoro compounds **12** and **13**[42] (Figure 4) were synthesized: first, to maintain the electron deficiency of the remaining carbonyl; and second, to determine if a parallel with work in the PTP1B inhibitor design area could be drawn. Specifically, phosphonomethyl phenylalanine (Pmp) is a nonhydrolyzable *p*Tyr mimic and inhibits PTP1B when incorporated into an appropriate peptide scaffold.[32,33] When phosphonodifluoromethyl phenylalanine (F_2Pmp) was substituted for Pmp, a 1000-fold increase in potency was observed.[34] Crystallography showed that this dramatic increase in potency may be attributable to an unconventional hydrogen bond between one of the fluorines and a phenylalanine amido group in the active site of the enzyme.[43] Compounds **12** and **13** gave no inhibition of CD45 at 10 μM.

Our analysis of the combined sets of actives and inactives led us to focus on compounds that possessed a six-membered near-planar ring containing a 1,2-dione; thus the chemistry focus would need to be incremental changes to the core structure. We restricted our synthetic efforts to compounds that would satisfy these requirements.

Proposed Mechanism of Action

As shown in Figure 5, it is hypothesized that the active site cysteine of CD45 attacks a carbonyl of the dione, thus rendering the enzyme catalytically inactive. At first glance, this mechanism is analogous to the inhibition of serine proteases by electrophilic carbonyl-based inhibitors.[44] The results indicate, however, that more than just a single electrophilic carbonyl group is required, as compounds **12** and **13** would be expected to inhibit the enzyme under the simplest variation of this scheme. There must be more to the inhibition; one hypothesis is that when the hemithioketal is flanked by a vicinal carbonyl group, as it is in the proposed covalent inhibitor-enzyme adduct, a thiophosphate ester transition state is mimicked. This hypothesis gave us a starting point from which to work.

Chemistry

The 4-aryl-substituted naphthalenediones were prepared according to Scheme 1. Suzuki couplings[45] with 4-bromo-1,2-naphthalenedione **14**[46] and various aryl boronic acids afforded **15**.

The nitrated phenanthrenediones **16** were synthesized via known methods as discussed in the Experi-

Scheme 2. Synthesis of Nitrogen-Substituted 9,10-Phenanthrenediones[a]

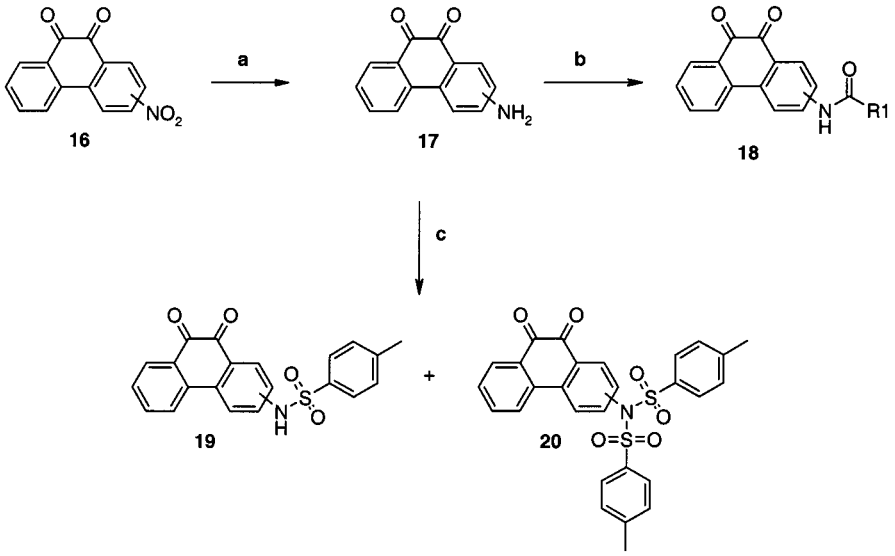

[a] Reagents: (a) Raney Ni, 50 psi H_2, THF; (b) R^1COCl, Na_2CO_3, THF; (c) TsCl, DMAP, Et_3N, CH_2Cl_2.

Scheme 3. Synthesis of Glycine-Derived Compounds[a]

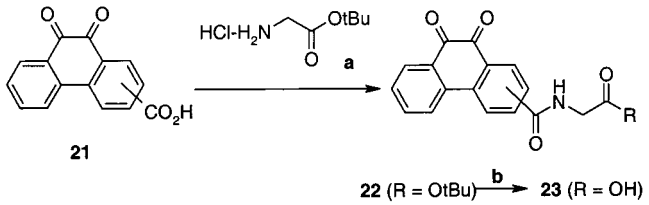

[a] Reagents: (a) EDC, DMAP, *i*Pr$_2$NEt, DMF; (b) TFA, CH_2Cl_2.

Scheme 4. Suzuki Coupling To Afford 2-Aryl-9,10-phenanthrenediones[a]

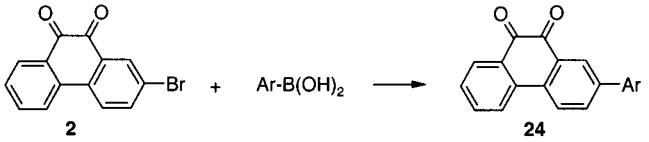

[a] Reagents: Pd_2dba_3, P(*o*-tol)$_3$, K_2CO_3, 10% H_2O−dioxane, 80 °C.

mental Section, and these were reduced to the amino compounds **17** using Raney nickel hydrogenation. These amino compounds were converted to the amides **18** and sulfonamides **19** and **20** using standard chemical transformations, Scheme 2.

The 9,10-phenanthrenedione-carboxylic acids **21**[47] were coupled with *tert*-butyl glycine hydrochloride to give **22**; in turn, a portion of the *tert*-butyl esters were hydrolyzed to the carboxylic acids **23**, Scheme 3.

2-Bromo-9,10-phenanthrenedione **2**[48] was used as a building block to assemble the 2-aryl-9,10-phenanthrenediones **24** via Suzuki couplings,[45] Scheme 4. Although this reaction was successfully run using various arylboronic acids, the utility of the products generated was limited. Only when the arylboronic acid was heterocyclic or ortho-substituted was the product sufficiently soluble for further evaluation.

The synthesis of the peptides in Scheme 5 begins with **3**, which was coupled with *N*-FMOC-L-asparagine *tert*-butyl ester to give **25**. The *tert*-butyl ester was hydrolyzed to the carboxylic acid, and this was attached to 2-chlorotrityl resin to give **26**. Standard solid-phase peptide chemistry was employed, followed by acetylation of the terminal nitrogen and cleavage off of the resin with TFA to afford **27**.

The solid-supported tetrapeptide fragments **28** seen in Scheme 6 were assembled using standard solid-phase peptide synthesis techniques. The fragments were coupled with the 9,10-phenanthrenedione-carboxylic acids **21** to give **29**. The 6-chlorochlortrityl resin link was then cleaved using TFA to afford the carboxy-linked peptides **30**.

Results and Discussion

The in vitro inhibitory activity of our compounds against the cytosolic portion of CD45 was evaluated initially using *p*NPP as the substrate and observing *p*-nitrophenol release.[49] The rate of CD45 inhibition by our compounds continued to change over the first 40 min of incubation as seen in Figure 6, suggesting a slow on-rate and/or a complex binding interaction.

Naphthalenediones. 1,2-Naphthalenedione, **6**, was identified as an inhibitor of CD45 in high-throughput

Scheme 5. Synthesis of Peptidyl 9,10-Phenanthrenediones[a]

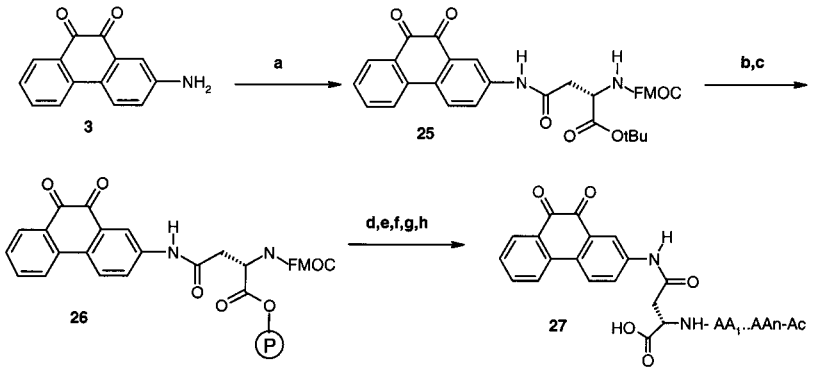

[a] Reagents: (a) FMOC-Asp-O*t*Bu, *N*-methylmorpholine, THF; (b) TFA, CH_2Cl_2; (c) *i*Pr$_2$NEt, 2-chlorochlortrityl resin, CH_2Cl_2−DMF; (d) piperidine, DMF; (e) FMOC-protected amino acid, HATU, *i*Pr$_2$NEt, DMF; (f) repeat steps d and e; (g) Ac_2O, *i*Pr$_2$NEt, DMF; (h) TFA, CH_2Cl_2.

Scheme 6. Synthesis of Carboxy-Linked Tetrapeptide Inhibitors[a]

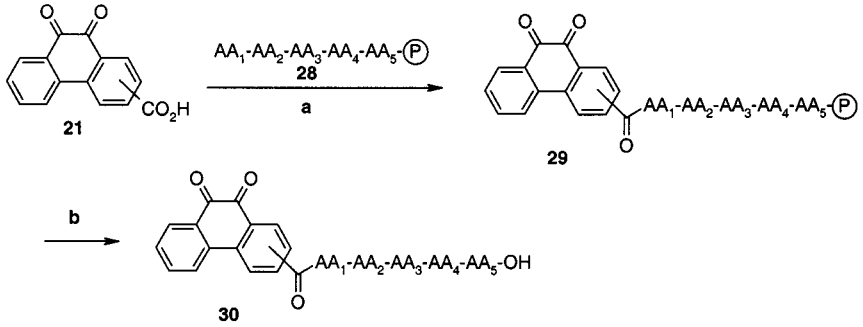

[a] Reagents: (a) HATU, *i*Pr$_2$NEt, DMF; (b) TFA.

Table 1. In Vitro Activity of the 1,2-Naphthalenediones[a]

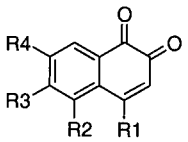

Compd	R1	R2	R3	R4	*p*NPP IC_{50}, μM	prolif. IC_{50}, μM	CC_{50}, μM
6	H	H	H	H	3 ± 0.5	7 ± 5.1	>30
31	NHPh	H	H	H	>30	ND[b]	ND
32	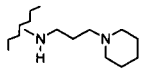	H	H	H	>30	ND	ND
33	$NH(CH_2)_2CO_2H$	H	H	H	>30	ND	ND
34	OCH_2CH_3	H	H	H	2 ± 0.2	>30	>30
35	$OCH_2CH{=}CH_2$	H	H	H	1.2 ± 0.3	>30	>30
14	Br	H	H	H	8.7 ± 1.0	22 ± 1.0	>30
36	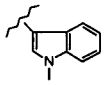	H	H	H	5 ± 2.7	1.5 ± 1.0	>30
37	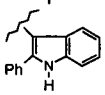	H	H	H	2.9 ± 0.5	2.2 ± 1.0	16 ± 7.1
38	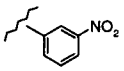	H	H	H	7.9 ± 2.7	0.4 ± 0.3	4 ± 1.6
39	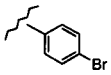	H	H	H	7.7 ± 1.6	0.2 ± 0.1	3 ± 2.1
40		H	H	H	5 ± 1.9	0.2 ± 0.1	12 ± 1.0
41	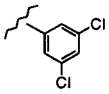	H	H	H	5.5 ± 1.6	0.3 ± 0.0	5.5 ± 1.2
42		H	H	H	8 ± 3.3	0.3 ± 0.0	12.4 ± 1.0
43	H	CO_2Me	H	H	11 ± 1.0	3.5 ± 1.3	>30
44	H	H	CO_2Me	H	7 ± 1.2	7.1 ± 2.0	>30
45	H	H	C(O)Ph	H	22 ± 5.0	11 ± 1.2	>30
46	H	H	H	OH	4.9 ± 0.3	>30	>30

[a] The reported values are the mean of all experiments, and the errors are standard errors of the mean. [b] ND = not determined.

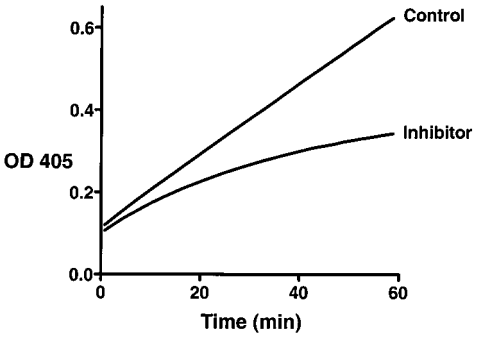

Figure 6. Kinetic analysis of the hydrolysis of *p*NPP by CD45 alone (control) or in the presence of 1.5 μM compound **2**. Note the curvature in the reaction progress curve which indicates the "slow-binding" nature of the inhibition of CD45 by the compound.

screening. It inhibited CD45 and T-cell inhibition in vitro in the single-digit micromolar range (Table 1). Furthermore, it was not toxic to T-cells at 30 μM. The 4-fold margin of inhibition of T-cell proliferation to cell cytotoxicity led us to expend chemistry efforts to further this series.

The known compounds **34** and **35** were analyzed to verify the surmised need for an electron-deficient carbonyl in our inhibitors.[50] Surprisingly, these two compounds are similarly potent to **6** in the enzyme inhibition assay, but inactive at inhibiting T-cell proliferation. Activity against the enzyme was surprising since all 12 compounds tested with a 4-amino substituent on the 1,2-naphthalenedione, including the three shown here in the table (**31**−**33**), did not inhibit *p*NPP hydrolysis by CD45 at 10 μM. We envisaged similar electronics between the 4-alkoxy- and 4-amino-1,2-naphthalenedione series and predicted, incorrectly, similar enzymatic activities. 4-Bromo-1,2-naphthalenedione **14**[46] was active at inhibiting CD45 with an IC_{50} of 8.7 μM but was only marginally active at inhibiting T-cell proliferation.

The known indoles **36** and **37**[51] were active against both the enzyme and T-cell proliferation. Both compounds had favorable ratios of cytotoxicity to cell

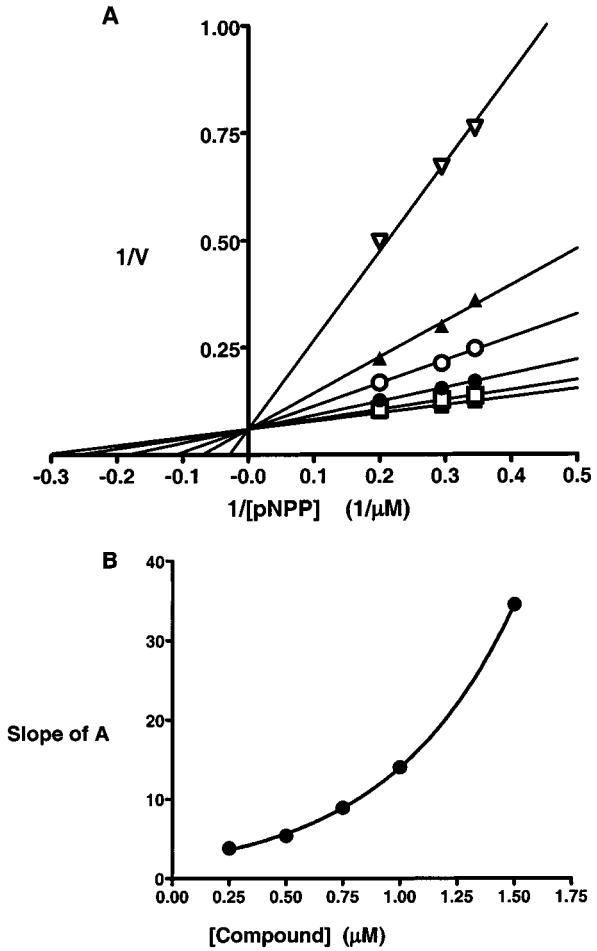

Figure 7. (A) Lineweaver−Burk analysis of CD45 inhibition by compound **5**. The activity of CD45 was measured at steady state as described in the Experimental Procedures section in the presence of the following concentrations of compound: ■, 0 μM; □, 0.25 μM; ●, 0.5 μM; ○, 0.75 μM; ▲, 1.0 μM; ▽, 1.5 μM. (B) Replot of the slope from the double-reciprocal plot versus concentrations of compound.

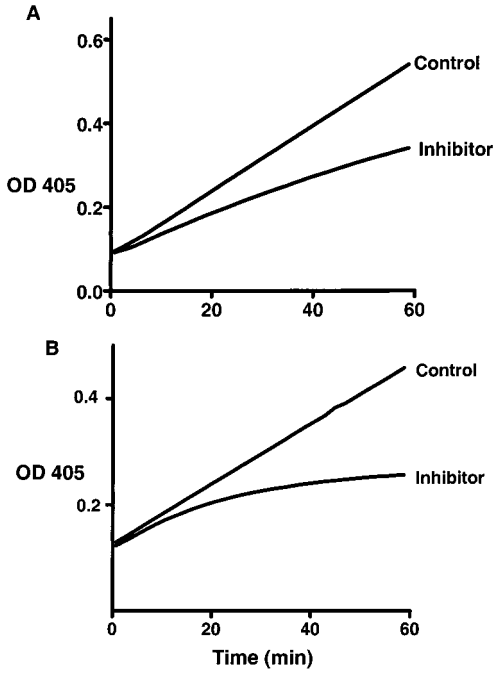

Figure 8. Kinetic analysis of the hydrolysis of *p*NPP by CD45 alone (control) or in the presence of 1.5 μM of compound **2**. (A) CD45 and compound were incubated for 90 min prior to the addition of *p*NPP. (B) *p*NPP and compound were incubated for 90 min prior to the addition of CD45. Note that preincubation of CD45 with compound reduced the curvature in the reaction progress curve consistent with the "slow-binding" nature of the inhibition of CD45 by the compound.

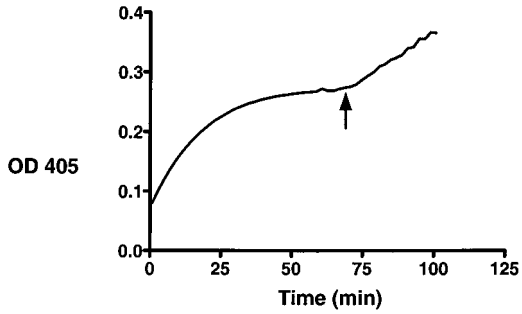

Figure 9. Reversible nature of CD45 inhibition by compound **4**. CD45 was incubated with 5 mM *p*NPP in the presence of compound, and the reaction was allowed to reach "steady state" kinetics. At 60 min, 10-fold excess *p*NPP was added to the reaction mixture to reverse inhibition.

proliferation (CC_{50}/IC_{50} proliferation), with 20- and 8-fold margins, respectively. Again, this positive result was unexpected considering the 3-position of indoles is electron-rich. This effect could be explained by the added aromaticity imparted by the indoles.

The 4-aryl-1,2-naphthalenediones **38**−**42**, synthesized to mimic the C ring of the 9,10-phenanthrenediones, displayed levels of enzyme inhibition similar to those of the other 1,2-naphthalenediones with no increase in potency against CD45 relative to **6**. On the other hand, the 4-aryl-1,2-naphthalenediones were among the most potent found at inhibiting T-cell proliferation. Even though cell cytotoxicity was observed in the sub-30 μM range, the ratios of cell cytotoxicity to inhibition of T-cell proliferation for this group of compounds ranged from as low as 18 to as high as 41.

The compounds **43**−**46** were also active against CD45 and displayed no cytotoxicity at 30 μM, and the subset of compounds **43**−**45** inhibited T-cell proliferation in the micromolar range. In general, based on our limited exploration, the 1,2-naphthalenedione series displayed a flat SAR against the isolated enzyme. The 1,2-naphthalenedione series was functionally active and displayed favorable cytoxicity characteristics; however, chemical stability might be an issue for both synthetic intermediates and final products in this series. Coupled with the fact that the 9,10-phenanthrenediones were more potent at inhibiting CD45, the stability issues led us to focus upon the 9,10-phenanthrenedione series.

9,10-Phenanthrenediones. Initially, a more detailed kinetic analysis of the compounds in the 9,10-phenanthrenedione series was undertaken. As shown in Figure 7A, the effect of these compounds on the CD45-catalyzed *p*NPP hydrolysis displayed the intersecting line pattern characteristic of a competitive inhibitor. However, the replot of the slope from the double-reciprocal plot versus compound concentration was hyperbolic, demonstrating a complex binding interaction and suggesting that the compound was not only competing at the substrate binding site (Figure 7B). This is similar to a report by Puius et al.[52] showing that *p*Tyr and bis-(*para*-phosphophenyl)methane substrates can

Table 2. Inhibitory Trend in a Series of Amino-9,10-phenanthrenediones[a]

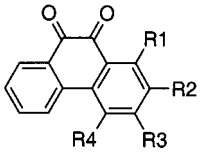

compd	R1	R2	R3	R4	*p*NPP IC_{50}, μM	*lck* IC_{50}, μM	prolif. IC_{50}, μM	CC_{50}, μM
47	NH_2	H	H	H	>30	>30	7.8 ± 0.8	9.6 ± 0.6
3	H	NH_2	H	H	0.4 ± 0.1	2.3 ± 0.9	0.2 ± 0.6	5.0 ± 1.0
48	H	H	NH_2	H	3.7 ± 1.5	10.5 ± 2.2	0.2 ± 0.1	17.0 ± 3.5
49	H	H	H	NH_2	0.8 ± 0.2	2.9 ± 1.5	0.2 ± 0.1	9.0 ± 2.0
50	$NHC(O)(CH_2)_2CO_2Me$	H	H	H	0.4 ± 0.1	4.7 ± 1.2	0.5 ± 0.2	9.0 ± 2.3
51	H	H	$NHC(O)(CH_2)_2CO_2Me$	H	0.4 ± 0.1	3.2 ± 0.7	1.0 ± 0.3	18.0 ± 2.5

[a] The reported values are the mean of all experiments, and the errors are standard errors of the mean.

interact with more than one site on PTP1B. In addition to occupying the canonical *p*Tyr-binding site (the active site), these substrate molecules also interact with a low-affinity noncatalytic aryl phosphate-binding site adjacent to the active site.

Preincubating CD45 with compound for 90 min before the addition of substrate resulted in a linear rate of *p*NPP hydrolysis as seen in Figure 8A. In contrast, preincubating compound with substrate for 90 min had no effect on the kinetics of substrate hydrolysis (Figure 8B). These findings further illustrate that these compounds are slow-binding inhibitors of CD45. It remains unresolved whether the compounds are undergoing hydration, there is a change in the conformation of the enzyme, and/or the compounds bind to multiple sites on the enzyme during the first 40 min of incubation.

To rule out the possibility that the phenanthrenediones were simply inactivating CD45 by direct or indirect oxidation of the catalytic cysteine residue, we conducted experiments to determine if the compounds were reversible inhibitors. The inhibition of CD45 by our compounds was completely reversed by addition of excess substrate (Figure 9). It should be emphasized that the renewed turnover of *p*NPP occurs readily even in the absence of additional reductant. This is in striking contrast to pervanadate, a commonly used inhibitor of PTPs, which is a potent oxidizing agent that causes irreversible inhibition of PTP1B.[53]

One of the first trends observed with the 9,10-phenanthrenedione series was the positional dependence of the amino-group effect, Table 2. 1-Amino-9,10-phenanthrenedione **47**, with an electron-donating amino group ortho-positioned to one of the carbonyls, is inactive against the isolated enzyme. The 2- and 4-amino-9,10-phenanthrenediones, **3** and **49**, where the meta-amino groups cannot be in resonance with the nearby carbonyl, are active with *p*NPP IC_{50}s in the submicromolar range. The conjugated para-position 3-amino group in **48** causes a loss of roughly an order of magnitude in potency relative to the two meta-positioned amino-substituted congeners **3** and **49**. Interestingly, when the 1- and 3-amino groups of **47** and **48** are converted into the electron-withdrawing succinamyl methyl esters **50** and **51**, the enzyme activity is restored.

No crisp parallel trend exists in the functional activity measurement opposite T-cell proliferation inhibition by these compounds. With the exception of **47**, all compounds in Table 2 are functionally active with submicromolar IC_{50}s. The 8 μM antiproliferative activity of **47**, in the absence of enzymatic activity, is explicable and attributable to the cytotoxicity of the compound. The other five compounds of Table 2 have safety margins between 18 and 85 with respect to the ratio of cytotoxicity to functional activity.

Many of the compounds were also evaluated in endpoint assays using a synthetic phosphotyrosyl peptide corresponding to phosphorylated lck^{505} [ATEGQ-**pY**QPQP] as the substrate.[54,55] This peptide corresponds to the negative regulatory *p*Tyr site of $p56^{lck}$ which is dephosphorylated by CD45 in vitro.[12] The same rank order of inhibitory capacity was observed when the *lck* 10-mer was used as substrate rather than *p*NPP, Table 2. Several lessons were learned from this small subset of compounds: (a) electron-donating groups in direct conjugation with the proximal carbonyl decrease or completely abolish inhibitory activity, which follows the hypothesized mechanism of inhibition; (b) the *lck* 10-mer data follow the same trend as *p*NPP data but are about 10-fold less potent; (c) inhibition of T-cell proliferation and cytotoxicity can be separated.

Results with a more diverse set of 9,10-phenanthrenediones are shown in Table 3. The introduction of a nitro group onto the phenanthrenedione core, namely compounds **4**, **5**, **52**, and **53,** gives compounds with enzymatic inhibitory capability that are similar to the parent 9,10-phenanthrenedione **1**. It was encouraging that the cytotoxicity of these compounds was lower than that of the parent structure. The 2,5-dinitro **54**, interestingly, is devoid of CD45 inhibitory activity, antiproliferative activity, and cytotoxicity.

Several carboxylic acid-substituted 9,10-phenanthrenediones were synthesized to potentially interact with the invariant Arg residue located at the active site. The carboxylic acids **55** and **56** were active against the enzyme but functionally inactive, presumably due to cell permeability issues. The glycine-derived carboxylic acids **57** and **58** maintained enzymatic activity, inhibited T-cell proliferation, and displayed no T-cell cytotoxicity at 30 μM. The *tert*-butyl ester **59** displayed a higher level of T-cell proliferation inhibition than its acid counterpart **57**, consistent with a neutral species' more facile passive diffusion across a membrane compared to its anionic counterpart.

Next a number of amides that reversed the position of the NH and C=O relative to what it had been in

Table 3. In Vitro Activity of the Phenanthrenediones[a]

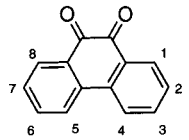

Compd	Substituent	POA[b]	*p*NPP IC_{50}, μM	prolif. IC_{50}, μM	CC_{50}, μM
1	-	-	0.7 ± 0.1	0.3 ± 0.2	1.3 ± 0.5
4	NO_2	2	2.4 ± 0.2	1.6 ± 0.4	10.0 ± 2.0
52	NO_2	3	0.5 ± 0.1	0.2 ± 0.0	2.8 ± 0.6
5	NO_2	4	0.5 ± 0.0	1.3 ± 0.2	10.0 ± 1.5
53	NO_2	2, 7	4.1 ± 0.6	0.5 ± .01	8.0 ± 2.5
54	NO_2	2, 5	>30	>30	>30
2	Br	2	0.4 ± 0.2	0.6 ± 0.5	5.0 ± 1.7
55	CO_2H	2	1.0 ± 0.2	>30	>30
56	CO_2H	3	1.0 ± 0.2	>30	ND[c]
57	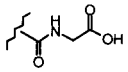	2	0.8 ± 0.3	4.4 ± 0.1	>30
58	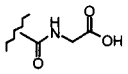	3	0.5 ± 0.1	6.5 ± 2.0	>30
59	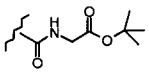	2	0.6 ± 0.1	0.4 ± 0.1	10 ± 2.0
60	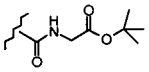	3	0.6 ± 0.0	0.32 ± 0.1	3.2 ± 0.9
61	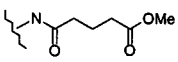	3	0.8 ± 0.1	1.6 ± 0.6	9.0 ± 2.3
62	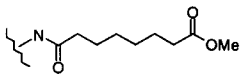	3	0.7 ± 0.0	1.3 ± 0.3	28.0 ± 1.1
63	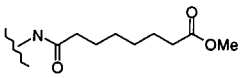	2	0.5 ± 0.2	1.3 ± 0.5	14.0 ± 4.0
64	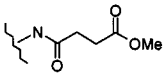	2, 7	0.5 ± 0.2	1.1 ± 0.4	7.0 ± 1.0
65	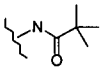	2	0.2 ± 0.1	0.1 ± 0.0	3.5 ± 1.0
66	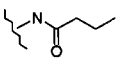	2	0.7 ± 0.3	1.1 ± 0.2	8.2 ± 2.9
67	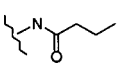	3	0.8 ± 0.4	0.8 ± 0.3	9.1 ± 2.2

Table 3 (Continued)

Compd	Substituent	POA[b]	*p*NPP IC_{50}, μM	prolif. IC_{50}, μM	CC_{50}, μM
19	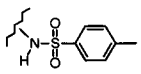	2	1.0 ± 0.0	6.4 ± 2.1	>30
20	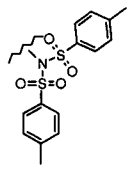	2	12.9 ± 1.2	0.8 ± 0.7	5.3 ± 1.6
68	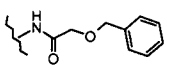	2	0.5 ± 0.3	1.0 ± 0.4	14.0 ± 2.5
69	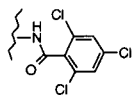	2	5.4 ± 0.3	1.3 ± 0.8	12.0 ± 2.2
70	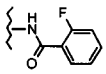	2	0.6 ± 0.2	3.1 ± 1.1	20.0 ± 2.5
71	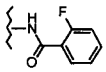	3	1.2 ± 0.2	2.9 ± 0.9	15.0 ± 1.7
72	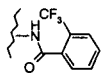	3	1.1 ± 0.0	1.5 ± 0.3	14.0 ± 1.6
73	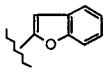	2	3.7 ± 2.1	0.8 ± 0.4	3.6 ± 0.9
74		2	0.8 ± 0.2	1.3 ± 0.1	8.4 ± 1.0
75		2	3.6 ± 1.5	0.7 ± 0.0	>30
76	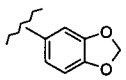	2	1.0 ± 0.2	1.7 ± 0.5	5.0 ± 0.1
77		2	1.0 ± 0.4	2.1 ± 0.2	9.5 ± 2.6
78		2	0.8 ± 0.2	1.7 ± 0.5	7.3 ± 1.0

[a] The reported values are the mean of all experiments, and the errors are standard errors of the mean. [b] POA = position of attachment. [c] ND = not determined.

compounds **57**−**60** and the two sulfonamides **19** and **20** were synthesized from 2- or 3-amino-9,10-phenanthrenedione. Among the amides made and tested were amide-ester variants, with a varying number of methylene spacer groups between the amide and the ester functionality (compounds **61**−**64**). In general, all these variants maintained the submicromolar enzyme inhibition of the of the glycine acids regardless of the number of methylene spacers introduced. Unfortunately, modest increases in inhibition of T-cell proliferation were offset by a parallel increase in cytotoxicity (below 30 μM).

Of the simple alkyl amides made, the pivalamide **65** is the most potent compound at inhibiting *p*NPP hydrolysis and T-cell proliferation, with IC_{50} values of 200 and 100 nM, respectively. Compound **65** also maintained a 35-fold margin in inhibition of proliferation over cytotoxicity. It should be noted that the alkyl amides and benzoyl amides (compounds **69**−**72**) inhibit CD45

Table 4. In Vitro Activity of Heterocyclic Analogues[a]

Compd	Structure	*p*NPP IC_{50}, μM	prolif. IC_{50}, μM	CC_{50}, μM
79	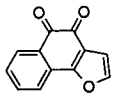	1.1 ± 0.1	0.6 ± 0.2	3.5 ± 0.4
80	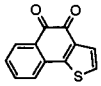	1.5 ± 0.2	0.6 ± 0.3	3.5 ± 1.0
81	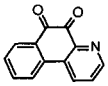	2.3 ± 0.7	0.4 ± 0.4	7 ± 1.7
82	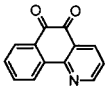	1.0 ± 0.4	0.2 ± 0.0	2.4 ± 1.6

[a] The reported values are the mean of all experiments, and the errors are standard errors of the mean.

with similar IC_{50}s. However, the alkyl amides were slightly more potent inhibitors of T-cell proliferation relative to the benzoyl amides.

A small subset of 2-aryl-9,10-phenanthrenediones **73**−**78** was also investigated. These possess IC_{50}s against the isolated enzyme and against T-cell proliferation in the 1 μM range, with variable cytotoxicity.

To improve the physical properties of the 9,10-phenanthrenediones, a few heterocyclic variants were made, Table 4. The furanyl-, thiophenyl-,[56] and pyridyl-[57] compounds **79**−**82** produced sustained CD45 inhibition, but they lost potency relative to **1**. They all maintained functional activity (inhibition of T-cell proliferation) while exhibiting variable cytotoxicity.

Peptidyl Inhibitors. As discussed previously, early PTP inhibitors focused on the incorporation of a nonhydrolyzable phosphotyrosine mimic into an appropriate peptide scaffold. In an attempt to increase the binding potency, various peptides were appended to the 9,10-phenanthrenedione core. The dione core was incorporated into peptides that correspond to the sequence Ala-Thr-Glu-Gly-Gln-***p*Tyr**-Gln-Pro-Gln-Pro surrounding the critical tyrosine residue in the *src* kinase $p56^{lck}$, a physiological substrate of CD45. Table 5 shows compounds where the peptide chain was built to the N-terminus of the *lck* peptide. These compounds inhibited CD45 in the single-digit micromolar range but were only marginally active or not active in inhibiting T-cell proliferation, presumably because of poor cellular permeability. Table 6 shows compounds where the peptide chain was appended to 2- or 3-carboxy-9,10-phenanthrenedione and progressed to the C-terminus of the *lck* peptide. More diversity was built into this subset of peptides, particularly those linked to the 2-carboxy, to take advantage of other potential recognition elements in the enzyme. These compounds, like the compounds in Table 5, were able to maintain, but not increase, potency against CD45. One interpretation of these results is that the amino acid residues do not make favorable contacts with the enzyme. On the other hand, no serious repulsions exist since enzyme inhibition is maintained. One interesting trend is noteworthy in compounds **88**−**105**, where the peptide chain is attached to 2-carboxy-9,10-phenanthrenedione: T-cell proliferation was inhibited by varying degrees. These compounds also show no cytotoxicity at 30 μM. In contrast, compounds **106**−**121**, those linked to the 3-position of the dione core (the most "*lck*-like"), have essentially lost functional activity.

Selectivity Studies. The large number of PTPs in the human body make it important to demonstrate selectivity for CD45 over other phosphatases. To examine this issue, the *lck* 10-mer was used as the substrate and a subset of phenanthrenediones were compared for activity against CD45 and PTP1B, a tyrosine phosphatase that is ca. 40% sequence homologous with CD45. The *lck* peptide was derived from the COOH terminus of $p56^{lck}$ (ATEGQ**pY**QPQP), a potential in vivo substrate of CD45.[58] This specific phosphopeptide has been used by others to characterize CD45 and other PTPases for specificity and selectivity.[55] In kinetic assays, the K_m of CD45 for *p*NPP, the substrate used in the initial studies, is 4.8 mM, with a catalytic efficiency, measured as k_{cat}/K_m, of 1.1×10^4 s^{-1} $M.^{-1}$ With the *lck* peptide as substrate, the K_m value changed to 130 μM and k_{cat}/K_m rises to 76×10^4 s^{-1} $M,^{-1}$ a vast improvement over *p*NPP.[55] However, the rank order potency of the compounds tested did not change with *lck* peptide substrate, giving us confidence that these inhibitors would block the activity of CD45 toward its physiological substrate.

The K_m of CD45 for the *lck* 10-mer was also determined using the end-point assay. In these assays, the ratio of *lck* to CD45 is about 3-fold higher than that used in the kinetic assays. The K_m value of CD45 for *lck* in this assay was 43 μM. The K_m values for PTP1B and FAP (Fas-associated phosphatase) for *lck* were similar to that obtained for CD45, with K_m values of 46 and 38 μM, respectively.

The first seven entries in Table 7 show that diversely substituted phenanthrenediones are inhibitors of CD45 with IC_{50}s in the single-digit micromolar range, while not inhibiting PTP1B. The 2-linked benzoyl amides **68** and **70**, however, inhibit both enzymes essentially equipotently. Compound **71**, which is merely a positional isomer of **70**, regains its CD45 activity and loses the PTP1B activity. The 2-aryl-9,10-phenanthrenediones **73**, **74**, and **77** show a reversal of selectivity, as these are now selective for PTP1B over CD45. The data in Table 7 demonstrate that, by making a simple structural modification (location or absence of an aryl group off of the 2-position), modulation of this series of inhibitors' selectivity for CD45 versus PTP1B is attainable. These findings follow what is known in the PTP1B inhibitor design area; Burke et al. showed that PTP1B has multiple binding interactions possible for polyaromatic systems.[39] It has also been shown more recently that the active site of PTP1B can accommodate substituted and extended aromatic systems, and these aromatic systems also interact beyond the catalytic site, which could lead to higher potency and phosphatase specificity.[35] This "plasticity" of PTP1B to allow binding of large hydrophobic groups seems to be attributable to the conformation of a single invariant amino acid residue at the active site.[59] Most of the non-peptide small-molecule inhibitors of PTP1B and other PTPs have an aromatic moiety as the core structure.

Table 5. In Vitro Activity of 9,10-Phenanthrenedione-Incorporated Peptidyl Inhibitors[a]

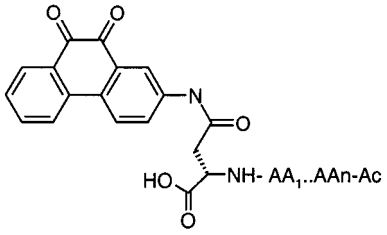

compd	AA_1..AAn-Ac	*p*NPP IC_{50}, μM	prolif. IC_{50}, μM	CC_{50}, μM
83	Gln	1.1 ± 0.2	>30	ND[b]
84	Gln-Gly-Glu	1.5 ± 0.3	>30	ND
85	Gln-Gly-Glu-Thr-Ala	2.0 ± 0.3	21.4 ± 2.5	ND
86	Gln-Gly-Glu-Thr-Ala-Thr	1.8 ± 0.3	23.0 ± 7.0	ND
87	Gln-Gly-Glu-Thr-Ala-Thr-Phe	1.4 ± 0.2	>30	ND

[a] The reported values are the mean of all experiments, and the errors are standard errors of the mean. [b] ND = not determined.

Table 6. In Vitro Activity of Additional Peptidyl Inhibitors[a]

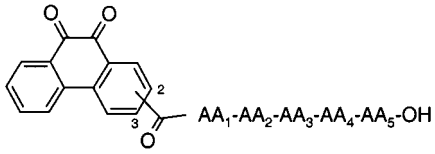

compd	POA[b]	AA_1-AA_2-AA_3-AA_4−AA_5	*p*NPP IC_{50}, μM	prolif. IC_{50}, μM	CC_{50}, μM	compd	POA[b]	AA_1-AA_2-AA_3-AA_4−AA_5	*p*NPP IC_{50}, μM	prolif. IC_{50}, μM	CC_{50}, μM
88	2	Gly-Gly-Pro-Glu-Gly	0.6 ± 0.3	19.3 ± 7.9	>30	**105**	2	Arg-Arg-Pro-Arg-Gly	1.3 ± 0.3	21.0 ± 8.7	>30
89	2	Glu-Gly-Pro-Glu-Gly	1.4 ± 0.0	8.8 ± 0.5	>30	**106**	3	Glu-Gln-Pro-Gln-Pro	0.6 ± 0.1	>30	>30
90	2	Arg-Gly-Pro-Glu-Gly	0.9 ± 0.0	3.3 ± 0.2	>30	**107**	3	Gly-Gln-Pro-Gln-Pro	1.2 ± 0.1	>30	>30
91	2	Gly-Glu-Pro-Glu-Gly	1.9 ± 0.3	9.0 ± 2.9	>30	**108**	3	Gln-Gln-Pro-Gln-Pro	0.7 ± 0.4	>30	>30
92	2	Glu-Glu-Pro-Glu-Gly	1.1 ± 0.0	14.2 ± 5.7	>30	**109**	3	Gly-Glu-Pro-Gln-Pro	0.7 ± 0.0	>30	>30
93	2	Arg-Glu-Pro-Glu-Gly	1.4 ± 0.2	5.0 ± 1.6	>30	**110**	3	Gln-Glu-Pro-Gln-Pro	1.1 ± 0.3	5.0 ± 2.4	>30
94	2	Gly-Arg-Pro-Glu-Gly	1.0 ± 0.6	5.5 ± 3.3	>30	**111**	3	Gly-Gln-Gly-Gln-Pro	1.1 ± 0.1	20.0 ± 1.8	>30
95	2	Glu-Arg-Pro-Glu-Gly	0.7 ± 0.1	3.0 ± 1.5	>30	**112**	3	Gln-Gln-Gly-Gln-Pro	0.9 ± 0.4	14.5 ± 7.2	>30
96	2	Arg-Arg-Pro-Glu-Gly	0.6 ± 0.2	11.0 ± 5.1	>30	**113**	3	Glu-Gln-Gly-Gln-Pro	0.6 ± 0.1	7.0 ± 2.5	>30
97	2	Gly-Gly-Pro-Arg-Gly	0.9 ± 0.3	16.0 ± 3.8	>30	**114**	3	Gly-Glu-Gly-Gln-Pro	0.7 ± 0.1	10.5 ± 3.2	>30
98	2	Glu-Gly-Pro-Arg-Gly	0.7 ± 0.1	23.0 ± 1.5	>30	**115**	3	Gln-Glu-Gly-Gln-Pro	1.1 ± 0.2	16.0 ± 10.3	>30
99	2	Arg-Gly-Pro-Arg-Gly	1.1 ± 0.2	14.0 ± 1.5	>30	**116**	3	Gln-Gln-Pro-Glu-Gly	0.9 ± 0.1	>30	ND[c]
100	2	Gly-Glu-Pro-Arg-Gly	0.8 ± 0.2	20.0 ± 2.5	>30	**117**	3	Gly-Gln-Gly-Glu-Pro	0.9 ± 0.01	>30	>30
101	2	Glu-Glu-Pro-Arg-Gly	1.0 ± 0.3	16.0 ± 6.7	>30	**118**	3	Gly-Gln-Pro-Gln-Gly	1.0 ± 0.1	>30	>30
102	2	Arg-Glu-Pro-Arg-Glu	0.9 ± 0.2	20.0 ± 5.5	>30	**119**	3	Gln-Gln-Pro-Gln-Gly	1.1 ± 0.1	>30	>30
103	2	Gly-Arg-Pro-Arg-Gly	1.4 ± 0.0	>30	>30	**120**	3	Gly-Glu-Pro-Gln-Gly	0.7 ± 0.0	>30	>30
104	2	Glu-Arg-Pro-Arg-Gly	0.8 ± 0.2	19.0 ± 5.1	>30	**121**	3	Gly-Gln-Pro-Glu-Gly	0.7 ± 0.1	>30	>30

[a] The reported values are the mean of all experiments, and the errors are standard errors of the mean. [b] POA = position of attachment. [c] ND = not determined.

Table 7. PTP1B Selectivity[a]

compd	CD45 *lck* IC_{50}, μM	PTP1B *lck* IC_{50}, μM
1	3.1 ± 1.2	>30
59	4.9 ± 1.5	>30
3	2.3 ± 0.9	>30
65	3.8 ± 0.3	>30
67	5.2 ± 2.6	>30
79	4.5 ± 2.8	>30
82	3.1 ± 0.7	>30
68	11.0 ± 0.9	18.0 ± 2.5
70	11.0 ± 5.2	18.0 ± 0.5
71	5.8 ± 2.0	>30
73	>30	19.0 ± 1.0
74	>30	18.0 ± 1.6
77	>30	16.0 ± 1.8

[a] The reported values are the mean of all experiments, and the errors are standard errors of the mean.

The selectivity seen between CD45 and PTP1B was very encouraging, but to further address the concern that the phenanthrenediones would be nonspecific and react with cysteine residues in general, a diverse subset of compounds was tested against proteases that have active site cysteine residues and also against another tyrosine phosphatase, FAP, as shown in Table 8. Although some compounds do show activity against cathepsin L and S, this is not seen for all compounds,

Table 8. Further Selectivity Data[a]

compd	CD45 *p*NPP IC_{50}	CD45 *lck* IC_{50}	FAP *p*NPP IC_{50}[b]	FAP *lck* IC_{50}[b]	cathep. B IC_{50}[b,c]	cathep. L IC_{50}[b,d]	cathep. S IC_{50}[b,e]
3	0.4	2.3	4.7	>30	>10	0.6	6.0
57	0.8	1.9	15	>30	>10	0.9	>10
64	0.3	2.9	12	>30	>10	5.4	>10
63	0.5	3.7	9.9	>30	>10	>10	>10
50	0.4	4.7	4.4	>30	>10	ND[f]	ND
70	0.6	11	0.6	20	>10	0.4	9
65	0.2	3.8	7	>30	>10	0.5	0.4
82	1.4	3.1	14	>30	>10	0.6	0.4

[a] All data are given in μM. [b] The value is the mean of experiments run in triplicate. [c] CBZ-L-lysine *p*-nitrophenyl ester used as substrate. [d] Z-Phe-Arg-NH-Mec used as substrate. [e] Z-Val-Val-Arg-NH-Mec used as substrate. [f] ND = not determined.

and none of the compounds tested were active against cathepsin B. The active site cysteine residue of cysteine proteases such as the cathepsins B, L, and S is readily oxidized, so these findings further support that the phenanthrenediones are not acting as oxidizing agents in the enzyme inhibition assays.[60] Likewise, with the exception of compound **70**, these compounds are far less potent against FAP when using either *p*NPP or the *lck* 10-mer as the substrate. These data, combined with the findings on PTP1B, indicate these compounds are not simple "thiol traps" and that it is possible to synthesize inhibitors with selectivity among tyrosine phosphatases.

In summary, a series of 9,10-phenanthrenediones has been developed that inhibit the protein tyrosine phosphatase CD45 and T-cell proliferation in the 1 μM range. These inhibitors were found to be reversible, competitive inhibitors of CD45-induced *p*NPP hydrolysis. Selectivity for CD45 over PTP1B is attainable by a simple structural modification, and selectivity for CD45 over FAP and three evaluated cysteine proteases is also achievable. The compounds presented in this paper are the most potent small-molecule inhibitors of CD45 known to date.

Experimental Section

Chemistry. ^{1}H NMR spectra were obtained at 300 MHz using a Bruker DPX 300 spectrometer and were referenced to TMS. Analytical HPLC was done on an HP 1100 HPLC, with a C_{18} Dynamax column (5 cm × 4.6 mm, 3 μM particle size, 100 Å pore size), and a flow rate of 0.5 mL/min, 20−60% CH_3CN in H_2O over 7.5 min, holding at 60% CH_3CN for 2.5 min, while monitoring at 254 and 210 nm. Mass spectral data were obtained on a Micromass QTOF mass spectrometer. Silica gel chromatography was performed with ICN silica 32−63, 60 Å. Thin-layer chromatography was done on silica gel 60 F-254 (0.25 mm thickness) plates, and visualization was accomplished with UV light. Elemental analyses (C, H, N) were performed on an Exeter Analytical CE-440 elemental analyzer, and all compounds are within ±0.4% of theory unless otherwise indicated. Unless otherwise noted, all materials were obtained commercially and used without further purification.

Compounds **1**, **6**, **31**, **32**, and **33** were purchased from commercial sources and used as received.

4-(2-Chloro-phenyl)-[1,2]naphthoquinone (42). To a solution of **14** (350 mg, 1.48 mmol) in THF (20 mL) and H_2O (5 mL) was added 2-chlorophenylboronic acid (231 mg, 1.48 mmol), followed by tri-*o*-tolylphosphine (45 mg, 148 μmol) and K_2CO_3 (614 mg, 4.44 mmol). The mixture was deoxygenated with bubbling N_2 for about 10 min, at which time the N_2 line was removed and tris(dibenzylideneacetone)dipalladium(0) (68 mg, 74 μmol) was added. The resultant mixture was heated to reflux for 2 h under N_2, at which point no starting bromide was detectable by TLC (hexanes:ethyl acetate, 1:1, v/v). The mixture was cooled to room temperature, and the THF evaporated under reduced pressure. The dried material was dissolved in ethyl acetate, washed sequentially with saturated aqueous ammonium chloride, H_2O, and brine, dried over Na_2SO_4, filtered, and evaporated under reduced pressure. The isolated material was chromatographed on silica gel (hexanes−ethyl acetate, 4:1, v/v) and dried to yield **42** as an orange solid: ^{1}H NMR (300 MHz, $CDCl_3$) δ 8.21 (1H, dd, J = 6.9, 2.1 Hz), 7.56−7.52 (3H, m), 7.48−7.44 (2H, m), 7.44 (1H, m), 6.91 (1H, dd, J = 2, 6 Hz), 6.39 (1H, s); HPLC 7.45 min. HRMS theor. [M + H]: 269.0369 amu; obs. [M + H]: 269.0366 amu; deviation of −1.4 ppm.

Compounds **38**−**41** were synthesized by the general procedure given for compound **42**. Please see the supporting material for characterization data.

Compounds **43**−**45** were prepared using the procedures as described by Barton et al.[61]

5,6-Dioxo-5,6-dihydro-naphthalene-1-carboxylic acid methyl ester (43): orange solid; ^{1}H NMR (300 MHz, $CDCl_3$) δ 8.62 (1H, d, J = 11 Hz), 8.29 (1H, d, J = 7.8 Hz), 8.20 (1H, d, J = 7.8 Hz), 7.58 (1H, t, J = 7.8 Hz), 6.56 (1H, d, J = 11 Hz), 3.99 (3H, s); HPLC 3.69 min. HRMS theor. [M + H]: 217.0501 amu; obs. [M + H]: 217.0518 amu; deviation of 7.9 ppm.

5,6-Dioxo-5,6-dihydro-naphthalene-2-carboxylic acid methyl ester (44): orange solid; ^{1}H NMR (300 MHz, $CDCl_3$) δ 8.17 (2H, m), 8.05 (1H, s), 7.52 (1H, d, J = 10.2 Hz), 6.53 (1H, d, J = 10.2 Hz), 3.99 (3H, s); HPLC 3.61 min.

6-Benzoyl-[1,2]naphthoquinone (45): orange solid; ^{1}H NMR (300 MHz, $CDCl_3$) δ 8.23 (1H, d, J = 7.8 Hz), 7.86 (1H, dd, J = 1.5, 7.8 Hz), 7.83−7.79 (3H, m), 7.67 (1H, m), 7.57−7.51 (3H, m), 6.54 (1H, d, J = 10.2 Hz); HPLC 5.93 min. HRMS theor. [M + H]: 263.0708 amu; obs. [M + H]: 263.072 amu; deviation of 4.5 ppm.

7-Hydroxy-[1,2]naphthoquinone (46). This compound was prepared by the method of Teuber and Goetz:[62] red solid; ^{1}H NMR (300 MHz, DMSO-d_6) δ 10.50 (1H, broad s), 7.56 (1H, d, J = 9.8 Hz), 7.40 (1H, d, J = 8.1 Hz, 7.31 (1H, d, J = 2.7 Hz), 7.05 (1H, dd, J = 8.1, 2.7 Hz), 6.16 (1H, d, J = 9.9 Hz). Anal. Calcd. for $C_{10}H_6O_3 \cdot 0.1H_2O$: C, 68.26; H, 3.55. Found: C, 67.96, 67.89; H, 3.64, 3.65.

Compounds **4**, **5**, **53**, and **54** were synthesized as described by Schmidt,[63] taking into account the results disclosed by Ray and Francis.[64]

2-Nitro-phenanthrene-9,10-dione (4): orange solid; ^{1}H NMR (300 MHz, DMSO-d_6) δ 8.80 (1H, d, J = 2.8 Hz), 8.69 (1H, d, J = 8.5 Hz), 8.60 (1H, dd, J = 2.4, 8.7 Hz), 8.51 (1H, d, J = 8.3 Hz), 8.22 (1H, dd, J = 1.4, 7.7 Hz), 7.93 (1H, ddd, J = 1.6, 8.1, 8.1 Hz), 7.73 (1H, dd, J = 7.5, 7.5 Hz). Anal. ($C_{14}H_7NO_4$) C, H, N.

4-Nitro-phenanthrene-9,10-dione (5): orange solid; ^{1}H NMR (300 MHz, DMSO-d_6) δ 8.27 (1H, dd, J = 1.5, 7.9 Hz), 8.17 (1H, dd, J = 1.3, 7.9 Hz), 8.10 (1H, dd, J = 1.5, 7.8 Hz), 7.79−7.71 (2H, m), 7.63 (1H, ddd, J = 0.9, 7.7, 7.7 Hz), 7.46 (1H, d, J = 8.0 Hz). Anal. ($C_{14}H_7NO_4 \cdot 0.25H_2O$) C, H, N.

2,7-Dinitro-phenanthrene-9,10-dione (53): yellow solid; ^{1}H NMR (300 MHz, tfashake-DMSO-d_6) δ 8.77 (2H, d, J = 2.7 Hz), 8.76 (2H, d, J = 9.1 Hz), 8.62 (2H, dd, J = 2.7, 9.1 Hz). Anal. ($C_{14}H_6N_2O_6$) C, H, N.

2,5-Dinitro-phenanthrene-9,10-dione (54): yellow solid; ^{1}H NMR (300 MHz, DMSO-d_6) δ 8.67 (1H, d, J = 2.5 Hz), 8.54 (1H, dd, J = 2.5, 9.1 Hz), 8.36 (1H, dd, J = 1.5, 8.1 Hz), 8.26 (1H, dd, J = 1.3, 7.8 Hz), 7.87 (1H, dd, J = 7.8, 7.8 Hz), 7.73 (1H, d, J = 8.8 Hz).

3-Nitro-phenanthrene-9,10-dione (52). This compound was prepared as described by Braithwaite and Holt:[65] orange solid; ^{1}H NMR (300 MHz, TFA-d_1−DMSO-d_6) δ 9.02 (1H, d, J = 1.7 Hz), 8.50 (1H, d, J = 8.1 Hz), 8.29 (2H, m), 8.13 (1H, dd, J = 1.1, 7.6 Hz), 7.85 (1H, ddd, J = 1.3, 7.7, 7.7 Hz), 7.64 (1H, dd, J = 7.4, 7.4 Hz). Anal. ($C_{14}H_7NO_4 \cdot 0.1H_2O$) C, H, N.

2,7-Diamino-phenanthrene-9,10-dione: Compound **53** (3.0 g, 10 mmol) was suspended in THF (200 mL), and Raney nickel (ca. 1 g) was added. The reaction was hydrogenated on a Parr shaker under 50 psi H_2 for 2.5 h, at which time the mixture was filtered through a plug of diatomaceous earth, and the filtrate was evaporated under rotary evaporation. The product was chromatographed on silica gel (15% to 100% EtOAc in CH_2Cl_2 as eluant) and dried to afford 2,7-diamino-phenanthrene-9,10-dione (1.1 g, 4.6 mmol, 46%) as a black solid. ^{1}H NMR (300 MHz, TFA-d_1−DMSO-d_6) δ 8.77 (2H, d, J = 2.7 Hz), 8.76 (2H, d, J = 9.1 Hz), 8.62 (2H, dd, J = 2.7, 9.1 Hz). Anal. Calcd for $C_{14}H_6N_2O_6$: C, 56.39; H, 2.02; N, 9.39. Found: C, 56.20, 56.44; H, 2.17, 2.14; N, 8.89, 8.95.

The compounds **3**, **47**, **48**, and **49** were synthesized from the appropriate nitro compound according to the general procedure given for 2,7-diamino-phenanthrene-9,10-dione.

2-Amino-phenanthrene-9,10-dione (3): black solid; ^{1}H NMR (300 MHz, DMSO-d_6) δ 8.00 (1H, d, J = 7.8 Hz), 7.92−7.87 (2H, m), 7.65 (1H, ddd, J = 1.7, 8.0, 8.0 Hz), 7.31 (1H,

dd, J = 7.0, 7.0 Hz), 7.19 (1H, d, J = 2.8 Hz), 6.91 (1H, dd, J = 2.5, 8.6 Hz), 5.87 (2H, s). Anal. ($C_{14}H_9NO_2 \cdot 0.33H_2O$) C, H, N.

1-Amino-phenanthrene-9,10-dione (47): purple solid; ^{1}H NMR (300 MHz, TFA-d_1−DMSO-d_6) δ 8.25 (1H, d, J = 8.2 Hz), 8.05 (1H, dd, J = 1.2, 7.8 Hz), 7.77 (1H, ddd, J = 1.5, 7.2, 8.6 Hz), 6.97 (1H, dd, J = 2.1, 7.4 Hz); HPLC 5.13 min. HRMS theor. [M + H]: 224.0712 amu; obs. [M + H]: 224.0718 amu; deviation of 2.9 ppm.

3-Amino-phenanthrene-9,10-dione (48): brown solid; ^{1}H NMR (300 MHz, DMSO-d_6) δ 7.99 (2H, m), 7.83 (1H, d, J = 8.4 Hz), 7.78 (1H, d, J = 7.2 Hz), 7.53 (1H, dd, J = 7.2, 7.2 Hz), 7.30 (1H, s), 6.89 (2H, s), 6.64 (1H, dd, J = 1.5, 8.6 Hz). Anal. ($C_{14}H_9O_2N \cdot 0.10H_2O$) C, H, N.

4-Amino-phenanthrene-9,10-dione (49): black solid; ^{1}H NMR (300 MHz, DMSO-d_6) δ 8.56 (1H, d, J = 8.0 Hz), 7.94 (1H, dd, J = 1.4, 7.8 Hz), 7.73 (1H, ddd, J = 1.6, 7.8, 7.8 Hz), 7.41 (1H, ddd, J = 1.0, 7.9, 7.9 Hz), 7.36 (1H, dd, J = 3.2, 5.9 Hz), 7.20 (2H, m), 5.84 (2H, s). Anal. ($C_{14}H_9NO_2$) C, H, N.

2-Bromo-phenanthrene-9,10-dione (2). This compound was prepared as described by Bhatt:[48] orange solid; ^{1}H NMR (300 MHz, DMSO-d_6) δ 8.30 (1H, d, J = 7.9 Hz), 8.27 (1H, d, J = 8.6 Hz), 8.07 (1H, d, J = 2.4 Hz), 8.04 (1H, d, J = 1.0, 7.6 Hz), 7.96 (1H, dd, J = 2.7, 8.9 Hz), 7.79 (1H, ddd, J = 1.7, 8.2, 8.2 Hz), 7.56 (1H, dd, J = 7.6, 7.6 Hz). Anal. ($C_{14}H_7O_2$) C, H.

Compounds **55** and **56** were prepared as described by Langenbeck et al.[47]

9,10-Dioxo-9,10-dihydro-phenanthrene-2-carboxylic acid (55): yellow solid; ^{1}H NMR (300 MHz, DMSO-d_6) δ 13.45 (1H, s), 8.51 (1H, d, J = 1.9 Hz), 8.46 (1H, d, J = 8.2 Hz), 8.37 (1H, d, J = 8.0 Hz), 8.24 (1H, dd, J = 2.0, 8.2 Hz), 8.08 (1H, dd, J = 0.75, 7.6 Hz), 7.83 (1H, dd, J = 7.2, 7.2 Hz), 7.61 (1H, dd, J = 7.5, 7.5 Hz). Anal. ($C_{15}H_8O_4 \cdot 0.4\ H_2O$) C, H.

9,10-Dioxo-9,10-dihydro-phenanthrene-3-carboxylic acid (56): orange solid; ^{1}H NMR (300 MHz, DMSO-d_6) δ 13.66 (1H, br s), 8.71 (1H, s), 8.35 (1H, d, J = 8.0 Hz), 8.12 (1H, d, J = 8.0 Hz), 8.08−8.02 (2H, m), 7.81 (1H, dd, J = 7.5, 7.5 Hz), 7.58 (1H, dd, J = 7.5, 7.5 Hz). Anal. ($C_{15}H_8O_4 \cdot 0.2H_2O$) C, H.

[(9,10-Dioxo-9,10-dihydro-phenanthrene-3-carbonyl)-amino]-acetic Acid *tert*-Butyl Ester (60). To a solution of **56** (1.1 g, 4.5 mmol) in anhydrous DMF (10 mL) under N_2 was added *tert*-butyl glycine hydrochloride (760 mg, 4.6 mmol), EDC (1.1 g, 6.0 mmol), DMAP (60 mg, 500 μmol), and diisopropylethylamine (2.1 mL, 12 mmol), and the resultant solution was stirred for 16 h. The reaction was diluted with EtOAc and washed with 1 M HCl, water, saturated aqueous $NaHCO_3$, and brine. The organic layer was dried over $MgSO_4$, filtered, concentrated, and chromatographed on silica gel (3:1 EtOAc:CH_2Cl_2, v/v) to afford a yellow solid (500 mg). This solid was subsequently recrystallized from refluxing EtOAc to afford pure **60** (310 mg, 31%): yellow solid; ^{1}H NMR (300 MHz, DMSO-d_6) δ 9.29 (1H, dd, J = 6.1, 6.1 Hz), 8.71 (1H, s), 8.38 (1H, d, J = 8.0 Hz), 8.13 (1H, d, J = 8.3 Hz), 8.07 (1H, dd, J = 1.5, 7.9 Hz), 7.97 (1H, dd, J = 1.5, 8.3 Hz), 7.85 (1H, ddd, J = 1.5, 7.8, 7.8 Hz), 7.58 (1H, ddd, J = 7.2, 7.2 Hz), 4.00 (2H, d, J = 6.1 Hz), 1.45 (9H, s). Anal. ($C_{21}H_{19}NO_5 \cdot 0.2H_2O$) C, H, N.

Compound **59** was prepared analogously to compound **60**.

[(9,10-Dioxo-9,10-dihydro-phenanthrene-2-carbonyl)-amino]-acetic acid *tert*-butyl ester (59): yellow solid; ^{1}H NMR (300 MHz, DMSO-d_6) δ 9.23 (1H, dd, J = 5.7, 5.7 Hz), 8.54 (1H, d, J = 1.9 Hz), 8.46 (1H, d, J = 8.7 Hz), 8.39 (1H, d, J = 7.9 Hz), 8.22 (1H, dd, J = 2.3, 8.7 Hz), 8.07 (1H, dd, J = 1.6, 7.7 Hz), 7.82 (1H, ddd, J = 1.5, 7.9, 7.9 Hz), 7.59 (1H, dd, J = 7.4, 7.4 Hz), 3.94 (2H, d, J = 6.3 Hz), 1.44 (9H, s). Anal. ($C_{21}H_{19}NO_5 \cdot 0.1H_2O$) C, H, N.

[(9,10-Dioxo-9,10-dihydro-phenanthrene-3-carbonyl)-amino]-acetic Acid (58). To a solution of **60** (200 mg, 550 μmol) in CH_2Cl_2 (10 mL) under N_2 was added TFA (10 mL). This mixture was stirred for 2 h and concentrated under reduced pressure. The residue was dissolved in CH_2Cl_2 and evaporated once again to rid residual TFA. The material was recrystallized from refluxing EtOAc to afford **58** (70 mg, 47%): orange solid; ^{1}H NMR (300 MHz, DMSO-d_6) δ 12.7 (1H, s), 9.29 (1H, dd, J = 5.7, 5.7 Hz), 8.71 (1H, s), 8.39 (1H, d, J = 7.9 Hz), 8.13 (1H, d, J = 8.3 Hz), 8.07 (1H, dd, J = 1.2, 7.5 Hz), 7.98 (1H, dd, J = 1.6, 8.2 Hz), 7.85 (1H, ddd, J = 1.3, 8.7, 8.7 Hz), 7.59 (1H, dd, J = 7.5, 7.5 Hz), 4.03 (2H, d, J = 5.6 Hz). Anal. ($C_{17}H_{11}NO_5 \cdot 1.0H_2O$) C, H, N.

Compound **57** was prepared analogously to compound **58**.

[(9,10-Dioxo-9,10-dihydro-phenanthrene-2-carbonyl)-amino]-acetic acid (57): orange solid; ^{1}H NMR (300 MHz, DMSO-d_6) δ 12.69 (1H, s), 9.22 (1H, dd, J = 6.0, 6.0 Hz), 8.54 (1H, d, J = 1.9 Hz), 8.46 (1H, d, J = 8.2 Hz), 8.39 (1H, d, J = 8.0 Hz), 8.23 (1H, dd, J = 1.9, 8.4 Hz), 8.08 (1H, dd, J = 1.1, 7.5 Hz), 7.82 (1H, ddd, J = 1.5, 8.0, 8.0 Hz), 7.59 (1H, dd, J = 8.0, 8.0 Hz), 3.97 (2H, d, J = 5.8 Hz). Anal. ($C_{17}H_{11}NO_5$) C, H, N.

***N*-(9,10-Dioxo-9,10-dihydro-phenanthren-2-yl)-2-fluoro-benzamide (70).** To a solution of **3** (50 mg, 240 μmol) in THF (10 mL) was added an excess of Na_2CO_3 (1 g), followed by 2-fluorobenzoyl chloride (46 μL, 384 μmol). The mixture was shaken overnight and then filtered, and the solvent evaporated. The resulting material was purified on a silica gel column, using CH_2Cl_2−10% EtOAC/CH_2Cl_2 as the eluant to yield the pure amide **70** as a red solid: ^{1}H NMR (300 MHz, DMSO-d_6) δ 10.80 (1H, s), 8.45 (1H, d, J = 2.4 Hz), 8.30 (1H, d, J = 9 Hz), 8.23 (1H, d, J = 8 Hz), 8.09 (1H, dd, J = 2.3, 8.9 Hz), 8.02 (1H, dd, J = 1.3, 7.7 Hz), 7.80−7.70 (2H, m), 7.62 (1H, m), 7.50 (1H, dd, J = 7.3, 7.3 Hz), 7.38 (2H, m); HPLC 6.97 min. HRMS theor. [M + H]: 346.0879 amu; obs. [M + H]: 346.0882 amu; deviation of 0.7 ppm.

Compounds **50**, **51**, **61**−**69**, **71,** and **72** were prepared analogously to the procedure used for the preparation of compound **70**. Please see the Supporting Information for characterization data.

***N*-(9,10-Dioxo-9,10-dihydro-phenanthrene-2-yl)-4-methyl-*N*-[(4-methylphenyl)sulfonyl]-benzenesulfonamide (20).** To a solution of **3** (200 mg, 900 μmol) in CH_2Cl_2 (10 mL) under N_2 was added Et_3N (630 μL, 4.48 mmol), *p*-toluenesulfonyl chloride (TsCl, 340 mg, 1.79 mmol), and a catalytic amount of *N*,*N*-(dimethylamino)pyridine. The resultant solution was stirred overnight, after which time it was diluted with ethyl acetate (25 mL) and washed sequentially with saturated aqueous NH_4Cl, water, and brine and then dried over Na_2SO_4. Filtration followed by evaporation under reduced pressure yielded a product which was purified by silica gel chromatography using CH_2Cl_2 as the eluant; the first material eluted from the column was the ditosylate **20** (39 mg, 73 μmol, 8%) which was dried to a yellow solid: ^{1}H NMR (300 MHz, DMSO-d_6) δ 8.39 (1H, d, J = 8.7 Hz), 8.31 (1H, d, J = 8.0 Hz), 8.06 (1H, dd, J = 1.2, 7.7 Hz), 7.81 (1H, dd, J = 7.5, 7.5 Hz), 7.73 (4H, d, J = 8.3 Hz), 7.60 (1H, dd, J = 7.5, 7.5 Hz), 7.54 (1H, m), 7.52 (4H, d, J = 8.3 Hz), 7.36 (1H, dd, J = 2.4, 8.5 Hz), 2.50 (6H, s); HPLC 9.85 min. HRMS theor. [M + H]: 532.0889 amu; obs. [M + H]: 532.087 amu; deviation of −3.5 ppm.

***N*-(9,10-Dioxo-9,10-dihydro-phenanthrene-2-yl)-4-methyl-benzenesulfonamide (19).** A second material which eluted from the column was the monotosylate **19** (53 mg, 140 mmol, 16%) which was dried to an orange solid: ^{1}H NMR (300 MHz, DMSO-d_6) δ 10.77 (1H, s), 8.17 (1H, d, J = 9 Hz), 8.12 (1H, d, J = 8.1 Hz), 7.96 (1H, dd, J = 1.5, 7.8 Hz), 7.78−7.29 (4H, m), 7.48 (1H, s), 7.46 (1H, t, J = 8.4 Hz), 7.38 (2H, d, J = 8.1 Hz), 2.32 (3H, s); HPLC 7.14 min. HRMS theor. [M + H]: 378.08 amu; obs. [M + H]: 378.0798 amu; deviation of −0.5 ppm.

2-Benzofuran-2-yl-phenanthrene-9,10-dione (73). To a mixture of **2** (150 mg, 520 μmol) in dioxane (5 mL) and H_2O (0.5 mL) were added benzo[*b*]furan-2-boronic acid (169 mg, 1.4 mmol), tris(dibenzylideneacetone)-dipalladium(0) (48 mg, 52 μmol), tri-*o*-tolylphosphine (32 mg, 1.4 mmol), and K_2CO_3 (220 mg, 1.57 mmol). The resultant mixture was heated at 80 °C for 18 h, and the solid material was removed by filtration. The soluble material was purified using a Rainin preparative HPLC on a Rainin phenyl column (25 cm × 21.4 mm, 8 μM particle size, 60 Å), 40 mL/min, with 50%−80% dioxane/H_2O for 40 min, followed by 80%−50% for 5 min. If the purity at this stage was not sufficient, the material was then chromato-

graphed on a silica gel column using CH_2Cl_2 as the eluant: purple solid; ^{1}H NMR (300 MHz, $CDCl_3$) δ 8.64 (1H, d, J = 1.8 Hz), 8.21 (2H, ddd, J = 1.2, 7.8, 7.8 Hz), 8.10 (1H, d, J = 8.7 Hz), 8.05 (1H, d, J = 7.8 Hz), 7.75 (1H, dd, J = 7.8, 7.8 Hz), 7.64 (1H, d, J = 7.5 Hz), 7.57 (1H, d, J = 8.1 Hz), 7.50 (1H, dd, J = 7.8, 7.8 Hz), 7.35 (1H, ddd, J = 1.2, 6.6, 6.6 Hz), 7.31−7.28 (2H, m); HPLC 10.97 min. HRMS theor. [M + H]: 325.0865 amu; obs. [M + H]: 325.0886 amu; deviation of 6.6 ppm.

Compounds **74**−**78** were prepared using the general procedure reported for compound **73**. Please see the Supporting Information for characterization details.

Compound 84. FMOCAsp(OH)OtBu (3.3 g, 8 mmol) and *N*-methylmorpholine (900 μL, 8 mmol) were dissolved in dry THF (20 mL) and chilled to −10 °C. Isobutylchloroformate (910 μL, 7 mmol) was added dropwise, maintaining the reaction temperature below −7 °C. To this mixture was added a suspension of **3** (1.12 g, 5 mmol) in dry THF (40 mL), and the reaction was allowed to warm to ambient temperature. The disappearance of **3** was monitored by TLC (R_f = 0.42, 25:75 EtOAc:CH_2Cl_2, v/v on a silica gel plate), and reaction was complete after 7 d. The solvent was removed by rotary evaporation, and the residue was partitioned between EtOAc and saturated aqueous NH_4Cl. The organic phase was washed with saturated aqueous $NaHCO_3$ and brine and then dried over anhydrous $MgSO_4$. This mixture was filtered, and the filtrate was concentrated to a red-brown solid and chromatographed on silica gel with 15:85, EtOAC:CH_2Cl_2, v/v. This gave FMOCAsp-2-aminophenanthrene-9,10-dione (1.92 g, 3.1 mmol, 63%) as a red solid. This intermediate was dissolved in CH_2Cl_2 (100 mL), and TFA (30 mL) was added. After 1 h the volatiles were removed by rotary evaporation. Residual TFA was removed by dissolving the material in CH_2Cl_2 and concentration on the rotary evaporator twice. This was dissolved in dry CH_2Cl_2 (100 mL), and diisopropylethylamine (5 mL) and dry DMF (10 mL) were added under N_2. 2-Chlorochlortrityl resin (4.5 g of 1.2 mmol/g, 5.5 mmol) was added to the mixture and mixed by shaking. After 3 h, MeOH (10 mL) was added, and the shaking was continued for an additional 10 min. The resin was collected by vacuum filtration and washed with CH_2Cl_2 (5 × 10 mL), DMF (2 × 10 mL), CH_2Cl_2 (2 × 10 mL), and MeOH (3 × 10 mL). The resin was dried for 64 h in vacuo. An incorporation of 2.3 mmol of FMOCAsp(3-aminophenanthrene-9,10-dione) was calculated based on the increase of mass to 5.8 g. The resin was swelled in DMF (25 mL) for 1 h and then washed with DMF (5 × 25 mL). The resin was treated with 20% piperidine in DMF (10 mL) for 3 min, drained, then was treated with more 20% piperidine in DMF (10 mL) for 7 min and drained. The resin was washed with DMF (10 × 10 mL). A solution of FMOCGln(trt)OH (6.72 g, 11 mmol), HATU (3.8 g, 10 mmol), and diisopropylethylamine (3.5 mL) in DMF (15 mL) was added to the resin and mixed with gentle nitrogen bubbling for 2 h. The solution was drained, and the resin was washed with DMF (10 × 10 mL). The resin was treated with 10 mL of 20% piperidine in DMF (10 mL) for 3 min and drained, and then another portion of 20% piperidine in DMF (10 mL) was added for 7 min and drained. The resin was washed with DMF (10 × 10 mL). A portion of the resin (ca. 10%) was removed for other reactions, and the remaining resin was treated with a solution of FMOCGlyOH (1.93 g, 11 mmol), HATU (3.8 g, 10 mol), and diisopropylethylamine (3.5 mL) in DMF (15 mL) for 1 h. The reaction was drained and washed with DMF (10 × 10 mL). The resin was treated with 20% piperidine in DMF (10 mL) for 3 min, drained, then treated with additional 20% piperidine in DMF (10 mL) for 7 min, and drained. The resin was washed with DMF (10 × 10 mL). A portion of the resin (about 10%) was removed for other reactions, and the remaining resin was treated with a solution of FMOCGlu(tBu)OH (4.68 g, 11 mmol), HATU (3.8 g. 10 mmol), and diisopropylethylamine (3.5 mL) in DMF (15 mL) for 16 h. The solution was drained, and the resin was washed with DMF (10 × 10 mL). The resin was treated with 20% piperidine in DMF (10 mL) for 3 min and drained, and then an additional 20% piperidine in DMF (10 mL) was added for 7 min and drained. The resin was washed with DMF (10 × 10 mL). A portion of this material (ca. 15%) was removed and treated with a solution of Ac_2O (1 mL) and diisopropylethylamine (2 mL) in DMF (5 mL) for 2 h. The solution was drained, washed with DMF (10 × 5 mL), CH_2Cl_2 (5 × 5 mL), and Et_2O (5 × 5 mL), and dried under a N_2 stream. The resin was treated with a solution of TFA containing 2% H_2O and 2% thioanisole (5 mL) for 2 h. The solids were removed, and the solution was concentrated to a red oil. Addition of Et_2O (10 mL) induced precipitation of a red solid, which was collected by vacuum filtration. The material was purified by preparative HPLC on a C_{18} Dynamax column (21.4 mm × 25 cm, 60 Å) using a gradient of 10% to 26% acetonitrile in H_2O with 0.1% TFA. Fractions containing pure product were combined and lyophilized to give the product **84** (40 mg) as a red solid: HPLC 2.69 min. HRMS theor. [M + H]: 695.2313 amu; obs. [M + H] 695.2307 amu; deviation of −0.9 ppm.

Compounds **83** and **85**−**87** were prepared in an analogous manner to compound **84.** Please see the Supporting Information for characterization data.

Compound 106. 6-Chlorochlortrityl resin (6.19 g, 7 mmol) was swelled in dry CH_2Cl_2 (30 mL), and a solution of FMOCprolineOH (1.18 g, 3.5 mmol) and diisopropylethylamine (1.8 mL, 10.5 mmol) in dry CH_2Cl_2 (10 mL) was added. The reaction was gently mixed under a nitrogen atmosphere for 30 min, and then MeOH (3 mL) was added to cap the unreacted sites. After 15 min, the resin was transferred to a fritted glass funnel and washed with DMF (2 × 50 mL), CH_2Cl_2 (2 × 50 mL), MeOH (2 × 50 mL), and Et_2O (2 × 50 mL). The resin was dried in vacuo at 50 °C to constant weight. A portion of this material (1.5 g, 0.25 mmol) was swelled in DMF (5 mL) for 15 min and then washed with DMF (3 × 5 mL). The resin was treated with 20% piperidine in DMF (5 mL) for 3 min, drained, and then treated with another 20% piperidine in DMF (5 mL) for 7 min and drained. The resin was washed with DMF (10 × 5 mL). A solution of FMOCglutamine(Trt)-OH (610 mg, 1 mmol), HATU (380 mg, 1 mmol), and diisopropylethylamine (350 μL) in DMF (5 mL) was added to the resin and mixed with a gentle nitrogen bubbling for 2 h. The solution was drained, and the resin was washed with DMF (10 × 5 mL). The resin was treated with 20% piperidine in DMF (5 mL) for 3 min and drained, and then another portion of 20% piperidine in DMF (5 mL) was added, mixed for 7 min, and then drained. The resin was washed with DMF (10 × 5 mL). A solution of FMOCprolineOH (340 mg, 1 mmol), HATU (380 mg, 1 mmol), and diisopropylethylamine (350 μL) in DMF (5 mL) was added to the resin and mixed with a gentle nitrogen bubbling for 16 h. The solution was drained, and the resin was washed with DMF (10 × 5 mL). The resin was treated with 20% piperidine in DMF (5 mL) for 3 min, drained, treated with another portion of 20% piperidine in DMF (5 mL) for 7 min, and drained. The resin was washed with DMF (10 × 5 mL). A solution of FMOCglutamineOH (370 mg, 1 mmol), HATU (380 mg, 1 mmol), and diisopropylethylamine (350 μL) in DMF (5 mL) was added to the resin and mixed with a gentle nitrogen bubbling for 2.5 h. The solution was drained and the resin washed with DMF (10 × 5 mL). The resin was treated with 20% piperidine in DMF (5 mL) for 3 min, drained, then treated with another 20% piperidine in DMF (5 mL) for 7 min, and drained. The resin was washed with DMF (10 × 5 mL). A solution of FMOCglutamateOH(OtBu) (830 mg, 1 mmol), HATU (380 mg, 1 mmol), and diisopropylethylamine (350 μL) in DMF (5 mL) was added to the resin and mixed with a gentle nitrogen bubbling for 2 h. The solution was drained, and the resin was washed with DMF (10 × 5 mL). The resin was treated with 20% piperidine in DMF (5 mL) for 3 min, drained, then treated with another 20% piperidine in DMF (5 mL) for 7 min, and drained. The resin was washed with DMF (10 × 5 mL). A solution of **56** (250 mg, 1 mmol), HATU (380 mg, 1 mmol), and diisopropylethylamine (350 μL) in DMF (5 mL) was added to the resin and mixed with a gentle nitrogen bubbling for 16 h. The solution was drained, and the resin was washed with DMF (10 × 5 mL), CH_2Cl_2 (5 × 5 mL), and Et_2O (5 × 5 mL) and then dried under a stream of N_2. The resin

was treated with TFA containing 2% thioanisole and 2% water (5 mL) for 3 h. The solids were filtered off, and the filtrate was evaporated to a red oil. Addition of Et_2O (10 mL) induced precipitation, and this solid was collected by vacuum filtration to give the product (300 mg) as a pink solid. The material was purified by preparative HPLC on a C_{18} Dynamax column (21.4 mm × 25 cm, 60 Å) using a gradient of 10% to 26% acetonitrile in water with 0.1% TFA. Fractions containing pure product were combined and lyophilized to give **106** (100 mg) as a yellow solid: HPLC 2.55 min. Anal. ($C_{40}H_{45}N_7O_{13}\cdot 1.0H_2O\cdot 0.5CF_3CO_2H$) C, H, N.

Compounds **88**−**105** and **107**−**121** were synthesized according to the general procedure given for compound **106**. Please see the Supporting Information for characterization data.

Biology. *p*NPP Assay for Phosphatase Activity. CD45 and PTP1B enzymes were purchased from BIOMOL (Plymouth Meeting, PA). FAP enzyme was obtained from BioSignal (Montreal, Canada). Phosphatase activity was assayed in 96-well plates in a buffer containing 20 mM imidazole, pH 7.0, 50 mM NaCl, 2.5 mM EDTA, 5 mM DTT, and 10 μg/mL BSA using *p*NPP as a substrate. In some experiments, 10 mM glutathione was substituted for DTT. Compounds were tested in a range from 30 to 0.01 μM, with a final concentration of 1 or 5% DMSO depending upon the solubility of the compound. PTPase activity was measured by following the increase in absorbance at 405 nm on a SpectraMax Plus spectrophotometric plate reader (Molecular Devices, Sunnyvale, CA).

Lck Peptide Assay for Phosphatase Activity. The *lck* COOH terminal peptide TEGQ*p*YQPQP was obtained from Cambridge Research Biochemicals (Wilmington, DE). Phosphatase activity was assayed in 96-well plates in a buffer containing 25 mM HEPES, pH 7.2, 5 mM DTT, and 10 μg/mL BSA using the *lck* peptide as a substrate. Compounds were tested in a range from 30 to 0.01 μM at a final concentration of 5% DMSO. Phosphatase enzyme was incubated with substrate, in the presence or absence of compound, at room temperature for 1.5 h. At the end of the incubation period, BIOMOL "Green Reagent" (BIOMOL), Plymouth Meeting, PA) was added to each well, the plates were incubated for 30 min at room temperature, and the absorbance was read at 620 nm. To estimate the K_m values for the different phosphatase enzymes, the *lck* 10-mer was varied over a concentration range of 25−600 μM. K_m values were calculated with GraphPad Prism software (GraphPad Software, San Diego, CA).

T-Cell Proliferation. Venous blood from healthy adult donors was collected into a sterile syringe containing 10 U/mL heparin. Peripheral blood mononuclear cells (PBMC) were isolated by density centrifugation on Lymphoprep (Nycomed Amersham, Oslo, Norway). The freshly isolated PBMC were washed, counted, and resuspended at 2×10^6 cells/mL in RPMI 1640 medium containing L-glutamine, 0.1 mg/mL gentamycin, and 10% heat inactivated human serum. PBMC were transferred to 96-well plates (2×10^5 cells/well) containing compound (0.01 to 30 μM) or vehicle control (0.3% DMSO) and incubated for 1 h before addition of the activating anti-CD3 antibody, OKT3 (30 ng/mL). After 24 h in culture, the cells were pulsed with [^{3}H]thymidine (1 μCi/well) overnight and harvested the next day onto 96-well Packard GF/C filter plates using a Packard Cell Harvester (Packard Instruments, Meriden, CT). Filter plates were counted on a Packard TopCount in Packard Microscint 20 scintillation fluid. IC_{50} values from enzyme and proliferation assays were calculated using GraphPad Prism software (GraphPad Software, San Diego, CA). Cyclosporine was routinely run as a positive control in all T-cell proliferation assays and exhibited an IC_{50} of 5.0 ± 1.2 nM ($n = 51$).

Cytotoxicity Assay. Calcein-AM (Molecular Probes, Eugene, OR) uptake, as a quantitative measure of cell viability, was used to evaluate the toxic effect of compounds on T-cells. Briefly, PBMC were treated for 3−7 days with 3−10 μg/mL PHA, a potent T-cell mitogen, to preferentially expand the T-cell population.[66]

The T-cell lymphoblasts were purified by separation over Lymphoprep, plated at 2×10^5/well in a round-bottom 96-well plate containing RPMI with compound and incubated overnight at 37 °C in an incubator containing 5% CO_2. The dilution scheme and culture media were the same as those used in the T-cell proliferation assay. After the incubation period, cells were washed with Dulbecco's phosphate- buffered saline (D-PBS) and incubated with 1 μM Calcein-AM for 30−45 min in D-PBS as described in the technical sheet provided with the LIVE/DEAD Viability/Cytotoxicity Kit from Molecular Probes. Percent viability was assessed on a fluorescent plate reader (excitation filter 485/20 nm; emission filter 530/25 nm) where the 100% control value is the fluorescence intensity observed in the absence of test compound. The results from this assay are expressed as CC_{50}, i.e., the concentration of compound that is cytotoxic for 50% of the cells. The CC_{50} was calculated using GraphPad Prism software (GraphPad Software, San Diego, CA). Methanol was used as a positive control (100% cytotoxicity) in these assays. Cyclosporine was not cytotoxic at 100 nM, the highest concentration tested in our assays.

Acknowledgment. We thank Paul Warwick for development of the synthesis of the *lck* 10-mer, Lisa Schaffter for the mass spectral analyses, Bruce Gomes for discussions of the kinetics of these compounds, and David Aharony, Smita Ghanekar, George Booth, and Nicola Clarkson for the cathepsin selectivity assays.

Supporting Information Available: Characterization data for compounds **38**−**41**, **50**, **51**, **61**−**69**, **71**, **72**, **74**−**78**, **83**, **85**−**105**, and **107**−**121**. This material is available free of charge via the Internet at http://pubs.acs.org.

References

(1) Mihatsch, M.; Kyo, M.; Morozumi, K.; Yamaguchi, Y.; Nickeleit, V.; Ryffel, B. The side-effects of cyclosporine-A and tacrolimus. *Clin. Nephrol.* **1998**, *49*, 356−363.
(2) Hojo, M.; Morimoto, M.; Maluccio, T.; Asano, T.; Morimoto, K.; Lagman, M.; Shimbo, T.; Suthanthiran, M. Cyclosporine induces cancer progression by a cell-autonomous mechanism. *Nature* **1999**, *397*, 530−534.
(3) Gijtenbeek, J.; van den Bent, M.; Vecht, C. Cyclosporine neurotoxicity: a review. *J. Neurol.* **1999**, *246*, 339−346.
(4) Zheng, X.-F.; Fiorentino, D.; Chen, J.; Crabtree, G. R.; Schreiber, S. L. TOR kinase domains are required for two distinct functions, only one of which is inhibited by rapamycin. *Cell* **1995**, *82*, 121−130.
(5) Morris, R. E. Rapamycins: antifungal, antitumor, antiproliferative and immunosuppressive macrolides. *Transplant Rev.* **1992**, *6*, 39−87.
(6) Groth, C. G.; Backman, L.; Morales, J. M.; Calne, R.; Kreis, H.; Lang, P.; Touraine, J. L.; Claesson, K.; Campistol, J. M.; Durand, D.; Wramner, L.; Brattstrom, C.; Charpentier, B. Sirolimus (rapamycin)-based therapy in human renal transplantation: similar efficacy and different toxicity compared with cyclosporine. Sirolimus Euuropean renal transplant study group. *Transplantation* **1999**, *15*, 1036−1042.
(7) Kaplan, M. J.; Ellis, C. N.; Bata-Csorgo, Z.; Kaplan, R. S.; Endres, J. L.; Fox, D. A. Systemic toxicity following administration of sirolimus (formerly rapamycin) for psoriasis: association of capillary leak syndrome with apoptosis of lesional lymphocytes. *Arch. Dermatol.* **1999**, *135*, 553−557.
(8) Andoh, T.; Burdmann, E.; Fransechini, N.; Houghton, D.; Bennett, W. Comparison of acute rapamycin nephrotoxicity with cyclosporine and FK506. *Kidney Int.* **1996**, *50*, 1110−1117.
(9) Hunter, T. Protein kinases and phosphatases: The yin and yang of protein phosphorylation and signaling. *Cell* **1995**, *80*, 225−236.
(10) Tonks, N. K.; Neel, B. G. From form to function: signaling by protein tyrosine phosphatase. *Cell* **1996**, *87*, 365−368.
(11) Zhang, Z.-Y. Protein-tyrosine phosphatases: biological function, structural characteristics, and mechanism of catalysis. *Crit. Rev. Biochem. Mol. Biol.* **1998**, *33*, 1−52.
(12) Trowbridge, I. S.; Thomas, M. L. CD45: an emerging role as a protein tyrosine phosphatase required for lymphocyte activation and development. *Annu. Rev. Immunol.* **1994**, *12*, 85−116.
(13) Weiss, A.; Littman, D. R. Signal transduction by lymphocyte antigen receptors. *Cell* **1994**, *76*, 263−274.
(14) Volarevic, S.; Burns, C. M.; Sussman, J. J.; Ashwell, J. D. Intimate association of Thy-1 and the T-cell antigen receptor with the CD45 tyrosine phosphatase. *Proc. Natl. Acad. Sci. U.S.A.* **1990**, *87*, 7085−7089.
(15) Pingel, J. T.; McFarland, E. C.; Thomas, M. L. Activation of CD45-deficient T cell clones by lectin mitogens but not anti-Thy-1. *Int. Immunol.* **1994**, *6*, 169−178.

(16) Prickett, T. C. R.; Hart, D. N. J. Anti-leukocyte common (CD45) antibodies inhibit dendritic cell stimulation of CD4 and CD8 T-lymphocyte proliferation. *Immunology* **1990**, *69*, 250−256.
(17) Lazarovits, A. I.; Poppema, S.; White, M. J.; Karsh, J. Inhibition of alloreactivity in vitro by monoclonal antibodies directed against restricted isoforms of the leukocyte-common antigen (CD45). *Transplantation* **1992**, *54*, 724−729.
(18) Lazarovits, A. I.; Poppema, S.; Zhang, Z.; Khandaker, M.; Le Feuvre, C. E.; Singhal, S. K.; Garcia, B. M.; Ogasa, N.; Jevnikar, A. M.; White, M. J.; Singh, G.; Stiller, C. R.; Zhong, R. Z. Prevention and reversal of renal allograft rejection by antibody against CD45RB. *Nature* **1996**, *380*, 717−720.
(19) Basadonna, G. P.; Auersvald, L.; Khuong, C. Q.; Zheng, X. X.; Kashio, N.; Zekzer, D.; Minozzo, M.; Qian, H.-Y.; Visser, L.; Diepstra, A.; Lavarovits, A. I.; Poppema, S.; Strom, T. B.; Rothstein, D. M. Antibody-mediated targeting of CD45 isoforms: a novel immunotherapeutic strategy. *Proc. Natl. Acad. Sci. U.S.A.* **1998**, *95*, 3821−3826.
(20) Burke, T. R., Jr.; Smyth, M.; Nomizu, M.; Otaka, A.; Roller, P. P. Preparation of fluoro- and hydroxy-4-(phosphonomethyl)-D,L-phenylalanine suitably protected for solid-phase synthesis of peptides containing hydrolytically stable analogues of *O*-phosphotyrosine. *J. Org. Chem.* **1993**, *58*, 1336−1340.
(21) Kole, H. K.; Akamatsu, M.; Ye, B.; Yan, X.; Barford, D.; Roller, P. P.; Burke, T. R., Jr. Protein-tyrosine phosphatase inhibition by a peptide containing the phosphotyrosyl mimetic L-O-malonyltyrosine. *Biochem. Biophys. Res. Commun.* **1995**, *209*, 817−822.
(22) Roller, P. P.; Wu, L.; Zhang, Z.-Y.; Burke, T. R., Jr. Potent inhibition of protein-tyrosine phopshatase 1B using the phosphotyrosyl mimetic fluoro-O-malonyl tyrosine (FOMT). *Bioorg. Med. Chem. Lett.* **1998**, *8*, 2149−2150.
(23) Moran, E. J.; Sarshar, S.; Cargill, J. F.; Shahbaz, M. M.; Lio, A.; Mjalli, A. M. M.; Armstrong, R. W. Radio frequency tag encoded combinatorial library method for the discovery of tripeptide-substituted cinnamic acid inhibitors of the protein tyrosine phosphatase PTP1B. *J. Am. Chem. Soc.* **1995**, *117*, 10787−10788.
(24) Burke, T. R., Jr.; Yao, Z.-J.; Zhao, H.; Milne, G. W. A.; Wu, L.; Zhang, Z.-Y.; Voigt, J. H. Enantioselective synthesis of non-phosphorus-containing phosphotyrosyl mimetic and their use in the preparation of tyrosine phosphatase inhibitory peptides. *Tetrahedron* **1998**, *54*, 9981−9994.
(25) Yao, Z.-J.; Ye, B.; Wu, X.-W.; Wang, S.; Zhang, Z.-Y.; Burke, T. R., Jr. Structure-based design and synthesis of small molecule protein-tyrosine phosphatase 1B inhibitors. *Bioorg. Med. Chem.* **1998**, *6*, 1799−1810.
(26) Ye, B.; Akamatsu, M.; Shoelson, S. E.; Wolf, G.; Giorgetti-Peraldi, S.; Yan, X.; Roller, P. P.; Burke, T. R., Jr. L-O-(2-malonyl)-tyrosine: a new phosphotyrosyl mimetic for the preparation of Src homology 3 domain inhibitory peptides. *J. Med. Chem.* **1995**, *38*, 4270−4275.
(27) Akamatsu, M.; Roller, P. P.; Chen, L.; Zhang, Z.-Y.; Ye, B.; Burke, T. R., Jr. Potent inhibition of protein-tyrosine phosphatase by phosphotyrosine-mimic containing cyclic peptides. *Bioorg. Med. Chem.* **1997**, *5*, 157−163.
(28) Groves, M. R.; Yao, Z.-J.; Roller, P. P.; Burke, T. R., Jr.; Barford, D. Structural basis for inhibition of the protein tyrosine phosphatase 1B by phosphotyrosine peptide mimetics. *Biochemistry* **1998**, *37*, 17773−17783.
(29) Taylor, S. D.; Kotoris, C. C.; Dinaut, A. N.; Wang, Q.; Ramachandran, C.; Huang, Z. Potent non-peptidyl inhibitors of protein tyrosine phosphatase 1B. *Bioorg. Med. Chem.* **1998**, *6*, 1457−1468.
(30) Desmarais, S.; Jia, Z.; Ramachandran, C. Inhibition of protein tyrosine phosphatases PTP1B and CD45 by sulfotyrosyl peptides. *Arch. Biochem. Biophys.* **1998**, *354*, 225−231.
(31) Ibrahimi, O. A.; Wu, L.; Zhao, K.; Zhang, Z.-Y. Synthesis and characterization of a novel class of protein tyrosine phosphatase inhibitors. *Bioorg. Med. Chem. Lett.* **2000**, *10*, 457−160.
(32) Zhang, Z.-Y.; Maclean, D.; McNamara, D. J.; Dobrusin, E. M.; Sawyer, T. K.; Dixon, J. E. Protein tyrosine phosphatase substrate specificity: size and phosphotyrosine positioning in peptide substrates. *Biochemistry* **1994**, *33*, 2285−2290.
(33) Chatterjee, S.; Goldstein, B. J.; Csermely, P.; Shoelson, S. E. Phosphopeptide substrates and phosphonopeptide inhibitors of protein-tyrosine phosphatases. In *Peptides*; Proceedings of the Twelfth American Peptide Symposium; Leiden: The Netherlands, 1992; pp 553−555.
(34) Burke, T. R., Jr.; Kole, H. K.; Roller, P. P. Potent inhibition of insulin receptor dephosphorylation by a hexamer peptide containing the phosphotyrosyl mimetic F_2Pmp. *Biochem. Biophys. Res. Commun.* **1994**, *204*, 129−134.
(35) Sarmiento, M.; Wu, L.; Keng, Y.-F.; Song, L.; Luo, Z.; Huang, Z.; Wu, G.-Z.; Yuan, A. K.; Zhang, Z.-Y. Structure-based discovery of small molecule inhibitors targeted to protein tyrosine phosphatase 1B. *J. Med. Chem.* **2000**, *43*, 146−155.
(36) Barford, D. J.; Flint, A. J.; Tonks, N. K. Crystal structure of human protein tyrosine phosphatase 1B. *Science* **1994**, *263*, 1397−1404.
(37) Wrobel, J.; Sredy, J.; Moxham, C.; Dietrich, A.; Li, Z.; Sawicki, D. R.; Seestaller, L.; Wu, L.; Katz, A.; Sullivan, D.; Tio, C.; Zhang, Z.-Y. PTP1B inhibition and antihyperglycemic activity in the ob/ob mouse model of novel 11-arylbenzo[*b*]naphtho[2,3-d]furans and 11-arylbenzo[*b*]naphtho[2,3-d]thiophenes. *J. Med. Chem.* **1999**, *42*, 3199−3202.
(38) Malamas, M. S.; Sredy, J.; Moxham, C.; Katz, A.; Xu, W.; McDevitt, R.; Adebayo, F. O.; Sawicki, D. R.; Seestaller, L.; Sullivan, D.; Taylor, J. R. Novel benzofuran and benzothiophene biphenyls as inhibitors of protein tyrosine phosphatase 1B with antihyperglycemic properties. *J. Med. Chem.* **2000**, *43*, 1293−1310.
(39) Burke, T. R., Jr.; Ye, B.; Yan, X.; Wang, S.; Jia, Z.; Chen, L.; Zhang, Z.-Y.; Barford, D. Small molecule interactions with protein-tyrosine phosphatase PTP1B and their use in inhibitor design. *Biochemistry* **1996**, *35*, 15989−15996.
(40) Iversen, L. F.; Andersen, H. S.; Branner, S.; Mortensen, S. B.; Peters, G. H.; Norris, K.; Olsen, O. H.; Jeppesen, C. B.; Lundt, B. F.; Ripka, W.; Moller, K. B.; Moller, N. P. H. Structure-based design of a low molecular weight, nonphosphorus, nonpeptide, and highly selective inhibitor of protein-tyrosine phosphatase 1B. *J. Biol. Chem.* **2000**, *274*, 10300−10307.
(41) Byon, J. C. H.; Kusari, A. B.; Kusari, J. Protein-tyrosine phosphatase-1B acts as a negative regulator of insulin signal transduction. *Mol. Cell. Biochem.* **1998**, *182*, 101−108.
(42) Zupan, M.; Jernej, I.; Stojan, S. Solvent effects in the fluorination of aromatic molecules with 1-chloromethyl-4-fluoro-1,4-diazoniabicyclo[2.2.2]octane bis(tetrafluoroborate). *J. Fluorine Chem.* **1995**, *70*, 7−8.
(43) Chen, L.; Wu, L.; Otaka, A.; Smyth, M. S.; Roller, P. P.; Burke, T. R., Jr.; den Hertog, J.; Zhang, Z.-Y. Why is phosphonodifluoromethyl phenylalanine a more potent inhibitory moiety than phosphonomethyl phenylalanine toward protein tyrosine phosphatases? *Biochem. Biophys. Res. Commun.* **1995**, *216*, 976−984.
(44) Leung, D.; Abbenante, G.; Fairlie, D. P. Protease inhibitors: current status and future prospects. *J. Med. Chem.* **2000**, *43*, 305−341.
(45) Miyaura, N.; Suzuki, A. Palladium-catalyzed cross-coupling reactions of organoboron compounds. *Chem. Rev.* **1995**, *95*, 2457−2483.
(46) Perumal, P. T.; Bhatt, M. V. Oxidation of halophenols and highly substituted phenols with lead(IV) acetate. *Synthesis* **1980**, 943−945.
(47) Langenbeck, W.; Schaller, R.; Arneberg, K. Uber organische katalysatoren, XXV. Mitteil. Katalytische wirkungen von o-chinonen. *Chem. Ber.* **1942**, *75*, 1483−1488.
(48) Bhatt, M. V. Evidence for a new type of substitution reaction of phenanthrene-9,10-quinone derivatives. *Tetrahedron* **1964**, *20*, 803−821.
(49) Zhang, Z.-Y.; Van Etten R. L. Pre-steady-state and steady-state kinetic analysis of the low molecular weight phosphotyrosyl protein phosphatase from bovine heart. *J. Biol. Chem.* **1991**, *266*, 1516−1525.
(50) Takuwa, A.; Soga, O.; Iwamoto, H. I.; Maruyama, K. The addition of alcohol to 1,2-naphthoquinone promoted by metal ions. A facile synthesis of 4-alkoxy-1,2-naphthoquinones. *Bull. Chem. Soc. Jpn.* **1986**, *59*, 2959−2961.
(51) Henrion, J.-C.; Jacquet, B.; Hocquaux, M.; Barre, G.; Hedayatullah, M.; Lion, C. Condensation indole/1,2-naphthoquinone. Recherche de conditions optimales dans la preparation d'une nouvelle serie de 4-(3-indolyl)-1,2-naphthoquinones. *Bull. Soc. Chim. Belg.* **1996**, *105*, 415−418.
(52) Puius, Y. A.; Zhao, Y.; Sullivan, M.; Lawrence, D. S.; Almo, S. C.; Zhang, Z.-Y. Identification of a second aryl phosphate-binding site in protein-tyrosine phosphatase 1B: A paradigm for inhibitor design. *Proc. Natl. Acad. Sci. U.S.A.* **1997**, *94*, 13420−13425.
(53) Huyer, G.; Liu, S.; Kelly, J.; Moffat, J.; Payette, P.; Kennedy, B.; Tsaprailis, G.; Gresser, M. J.; Ramachandran, C. Mechanism of inhibition of protein-tyrosine phosphatases by vanadate and pervanadate. *J. Biol. Chem.* **1997**, *272*, 843−851.
(54) Harder, K. W.; Owen, P.; Wong, L. K. H.; Aebersold, R.; Clark-Lewis, I.; Jirik, F. R. Characterization and kinetic analysis of the intracellular domain of human protein tyrosine phosphatase β (HPTPβ) using synthetic phosphopeptides. *Biochem. J.* **1994**, *298*, 395−401.
(55) Cho, H.; Krishnaraj, R.; Itoh, M.; Kitas, E.; Bannwarth, W.; Saito, H.; Walsh, C. T. Substrate specificities of catalytic fragments of protein tyrosine phosphatases (HPTPβ, LAR, and CD45) toward phosphotyrosylpeptide substrates and thiophosphotyrosylated peptides as inhibitors. *Protein Sci.* **1993**, *2*, 977−984.

(56) Brandao, M. A. F.; deOliveira, A. B.; Snieckus, V. Cross coupling strategies. A regiospecific route to heteroring-annelated *ortho*-naphthoquinones and a short synthesis of *β*-lapachone. *Tetrahedron Lett.* **1993**, *34*, 2437−2440.
(57) Braven, J.; Hanson, R. W.; Smith, N. G. Synthetic routes to indenopyridine analogues of morphactins. *J. Heterocycl. Chem.* **1995**, *32*, 1051−1056.
(58) Hurley, T. R.; Hyman, R.; Sefton, B. M. Differential effects of expression of the CD45 tyrosine protein phosphatase on the tyrosine phosphorylation of the lck, fyn, and c-src tyrosine protein kinases. *Mol. Cell. Biol.* **1993**, *13*, 1651−1656.
(59) Sarmiento, M.; Puius, Y. A.; Vetter, S. W.; Keng, Y.-F.; Wu, L.; Zhao, Y.; Lawrence, D. S.; Almo, S. C.; Zhang, Z.-Y. Structural basis of plasticity in protein tyrosine phosphatase 1B substrate recognition. *Biochemistry* **2000**, *39*, 8171−8179.
(60) Chapman, H. A.; Riese, R. J.; Shi, G.-P. Emerging roles for cysteine proteases in human biology. *Annu. Rev. Physiol.* **1997**, *59*, 63−88.
(61) Barton, D. H. R.; Brewster, A. G.; Ley, S. V.; Read, C. M.; Rosenfeld, M. N. Oxidation of phenols, pyrocatechols, and hydroquinones to *ortho*-quinones using benzeneseleninic anhydride. *J. Chem. Soc., Perkin Trans. 1* **1981**, 1473−1476.
(62) Teuber, H.-J.; Goetz, N. Reaktionen mit nitrosodisulfonat,V. Mittel.: Uber die bildung von naphthochinon. *Chem. Ber.* **1954**, *87*, 1236−1251.
(63) Schmidt, J. Nitroderivate des phenanthrenchinons. *Chem. Ber.* **1903**, *23*, 3726−3730.
(64) Ray, F. E.; Francis, W. C. Polynitro compounds of fluorene. *J. Org. Chem.* **1943**, *8*, 52−59.
(65) Braithwaite, R. S. W.; Holt, P. F. The nitration of 9-bromophenanthrene. *J. Chem. Soc.* **1959**, 2304−2305.
(66) Bradley, L. M. Cell Poliferation. In *Selected Methods in Cellular Immunology*; Mishell, B. B., Shiigi, S. M., Eds.; W. H. Freeman and Co.: San Francisco, 1980.

JM000447I